Journal of Virology®

VIRUS-CELL INTERACTIONS

Porcine Mx1 Protein Inhibits Classical Swine Fever Virus Replication by Targeting Nonstructural Protein NS5B

Jing Zhou,[a] Jing Chen,[a] Xiao-Min Zhang,[c] Zhi-Can Gao,[a] Chun-Chun Liu,[a] Yun-Na Zhang,[a] Jin-Xiu Hou,[a] Zhao-Yao Li,[a] Lin Kan,[a] Wen-Liang Li,[b] Bin Zhou[a]

[a]College of Veterinary Medicine, Nanjing Agricultural University, Nanjing, China
[b]Institute of Veterinary Medicine, Jiangsu Academy of Agricultural Sciences, Nanjing, China
[c]Rugao Animal Husbandry and Veterinary Station, Rugao, China

ABSTRACT Mx proteins are interferon (IFN)-induced GTPases that have broad antiviral activity against a wide range of RNA and DNA viruses; they belong to the dynamin superfamily of large GTPases. In this study, we confirmed the anti-classical swine fever virus (CSFV) activity of porcine Mx1 *in vitro* and showed that porcine Mx2 (poMx2), human MxA (huMxA), and mouse Mx1 (mmMx1) also have anti-CSFV activity *in vitro*. Small interfering RNA (siRNA) experiments revealed that depletion of endogenous poMx1 or poMx2 enhanced CSFV replication, suggesting that porcine Mx proteins are responsible for the antiviral activity of interferon alpha (IFN-α) against CSFV infection. Confocal microscopy, immunoprecipitation, glutathione *S*-transferase (GST) pulldown, and bimolecular fluorescence complementation (BiFC) demonstrated that poMx1 associated with NS5B, the RNA-dependent RNA polymerase (RdRp) of CSFV. We used mutations in the poMx1 protein to elucidate the mechanism of their anti-CSFV activity and found that mutants that disrupted the association with NS5B lost all anti-CSV activity. Moreover, an RdRp activity assay further revealed that poMx1 undermined the RdRp activities of NS5B. Together, these results indicate that porcine Mx proteins exert their antiviral activity against CSFV by interacting with NS5B.

IMPORTANCE Our previous studies have shown that porcine Mx1 (poMx1) inhibits classical swine fever virus (CSFV) replication *in vitro* and *in vivo*, but the molecular mechanism of action remains largely unknown. In this study, we dissect the molecular mechanism of porcine Mx1 and Mx2 against CSFV *in vitro*. Our results show that poMx1 associates with NS5B, the RNA-dependent RNA polymerase of CSFV, resulting in the reduction of CSFV replication. Moreover, the mutants of poMx1 further elucidate the mechanism of their anti-CSFV activities.

KEYWORDS antivirus, classical swine fever virus (CSFV), mutants, nonstructural protein 5B (NS5B), porcine Mx1 (poMx1)

Classical swine fever (CSF), caused by CSF virus (CSFV), is an epidemic disease that affects the pig industry worldwide, particularly in China (1). Although the C strain is one of the most effective vaccines against CSFV, this vaccine cannot be used in the European Union (EU) because it is impossible to serologically differentiate vaccinated from infected pigs (2, 3). In addition, since any vaccine needs time to take effect (4), pigs can still be infected after vaccination before protective antibodies appear. Novel antiviral strategies are needed to reduce the losses from CSF (5).

Mx proteins are interferon (IFN)-induced dynamin-like GTPases that are present in all vertebrates and have a broad range of antiviral activities against a broad range of viruses (6, 7). Sequence alignments show that Mx GTPases have an N-terminal GTPase (G) domain, a middle domain (MD), and a C-terminal GTPase effector domain (GED) in common with dynamin, but they lack a pleckstrin homology (PH) domain and a

Received 8 December 2017 **Accepted** 9 January 2018

Accepted manuscript posted online 17 January 2018

Citation Zhou J, Chen J, Zhang X-M, Gao Z-C, Liu C-C, Zhang Y-N, Hou J-X, Li Z-Y, Kan L, Li W-L, Zhou B. 2018. Porcine Mx1 protein inhibits classical swine fever virus replication by targeting nonstructural protein NS5B. J Virol 92:e02147-17. https://doi.org/10.1128/JVI.02147-17.

Editor Bryan R. G. Williams, Hudson Institute of Medical Research

Address correspondence to Bin Zhou, zhoubin@njau.edu.cn.

J.Z. and J.C. contributed equally to this work.

proline-rich domain (8, 9). It has been well established that the dynamin-like GTPase activity, including GTP binding and GTP hydrolysis, is required for Mx proteins to function (10, 11). The antiviral profile of Mx proteins is influenced to some extent by their subcellular localization (12, 13). Different Mx proteins associate with distinct intracellular compartments in the cytoplasm and nucleus. However, the significance of these associations for antiviral activity is not always obvious. The molecular mechanism behind this broad yet specific antiviral action is not fully understood, but recent work on Mx structure and evolution is providing new insights (14, 15). In particular, studies of human MxA (huMxA) and huMxB, which share 63% sequence identity (16, 17), have shed light on the relationship between intracellular localization, transport function, and antiviral activity. Research has revealed an increasing number of RNA and DNA viruses that are inhibited by huMxA (16). Although HIV-1 is not among them, a broad screen for IFN-induced anti-HIV-1 factors revealed that huMxB inhibits HIV-1 and other primate lentiviruses (17, 18). A large body of evidence suggests that the known antiviral Mx GTPases have intrinsic activity and interact with viral components, inhibiting viruses at various stages in their life cycle (7). Therefore, Mx GTPases appear to recognize specific viral components that enter the cell upon infection or are produced in infected cells shortly thereafter.

Two Mx genes have been reported in pigs and designated *Mx1* and *Mx2* (19). The full-length porcine Mx1 (poMx1) gene (1,992 bp) was first isolated from the German Landrace breed and mapped to chromosome 13 (20, 21). Based on nucleotide and amino acid sequences, poMx1 and poMx2 are closely homologous to huMxA and huMxB (16), suggesting that the poMx proteins have similar antiviral functions. Likewise, previous studies have shown that functional huMxA and poMx1 are located in the cytoplasm of target cells and exhibit similar antiviral activities against vesicular stomatitis virus (VSV) (22), influenza A virus (FLUAV) (23), and CSFV (24–26). Furthermore, recent studies have shown that poMx1 inhibits the replication of foot-and-mouth disease virus (FMDV) and bovine viral diarrhea virus (BVDV) (27, 28). However, our research has shown that neither poMx1 nor poMx2 is responsible for the antiviral activity of IFN-α against Japanese encephalitis virus (JEV) (29). Our work has shown that wild-type (WT) poMx1 inhibits CSFV replication although the molecular mechanism of the inhibition remains to be elucidated. Also, whether poMx2 also inhibits CSFV replication remains an unanswered question.

To characterize the mechanism of poMx1 in viral inhibition, a series of mutants was constructed using the huMxA mutants as guidelines for design, and the mutants as well as wild-type poMx1, poMx2 huMxA, and mmMx1 were subsequently expressed in PK-15 cells. We found that porcine Mx proteins do not affect CSFV entry into PK-15 cells but do interact with CSFV NS5B. Further, colocalization, coimmunoprecipitation (co-IP), glutathione *S*-transferase (GST) pulldown, and bimolecular fluorescence complementation (BiFC) experiments clearly indicated that poMx1 (WT, L618D, or E646R) and NS5B form a complex and that the interaction between Mx protein and NS5B occurs in the cytoplasm.

RESULTS

Overexpression of Mx proteins. The plasmids pcDNA-poMx1-HA (WT and mutant poMx1; HA is hemagglutinin), pcDNA-poMx2-HA, pcDNA-huMxA-HA, pcDNA-mmMx1-HA, and pcDNA3.0 were transfected into PK-15 cells and maintained for 48 h. Western blotting with anti-HA monoclonal antibody (MAb) revealed an approximately 74- to 82-kDa band in the lysates of transfected cells (Fig. 1A); this band was absent in the lysate of the vector control (lane 10). The oligomerization state of Mx proteins was assessed using nondenaturing PAGE (Fig. 1B). As expected, the WT Mx proteins were tetrameric. The mutants poMx1 (K83A), poMx1 (L618D), and poMx1 (E646R) were also tetrameric. However, the mutants poMx1 (R409D) and poMx1 with a deletion of residues 534 to 573 (ΔL4) were tetrameric, dimeric, and monomeric, indicating that they have three oligomeric forms. The M527D mutation in huMxA renders the protein incapable of forming oligomers, resulting in only a monomer form (9). The same

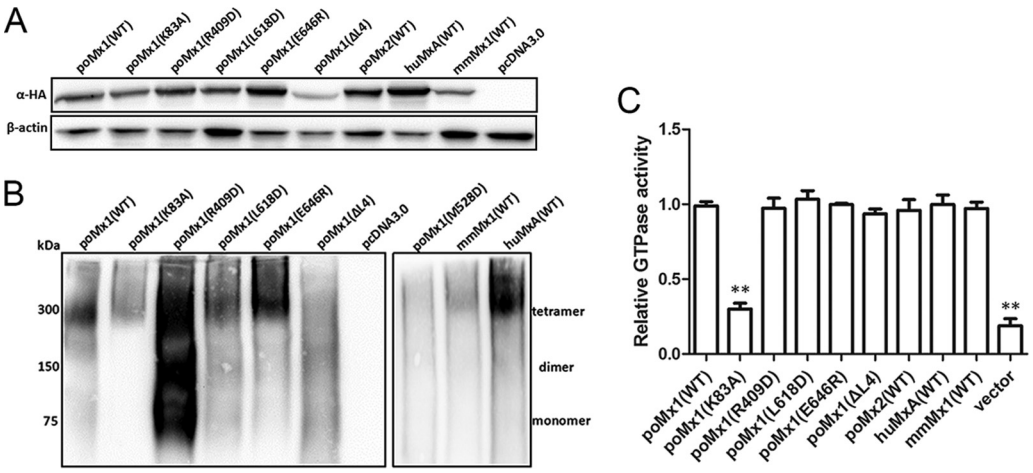

FIG 1 Expression of Mx proteins in PK-15 cells. (A) Western blotting of lysates from cells transfected with plasmids encoding HA-tagged poMx1 (WT or mutants), huMxA (WT), poMx2 (WT), or mmMx1 (WT) and then probed with rabbit anti-HA MAb and anti-β-actin MAb. (B) Western blotting of lysates run on a nondenaturing PAGE gel from cells transfected with plasmids encoding poMx1 (WT or mutants), huMxA (WT), or mmMx1 (WT) and then probed with rabbit anti-HA MAb. (C) GTPase activity of Mx proteins. Cells transfected with the plasmids named above and grown for 48 h were washed with ddH_2O and lysed in radioimmunoprecipitation assay buffer with sonication. GTPase activity of the cell lysates was determined using a QuantiChrom ATPase/GTPase assay kit. Results are presented as the means $\pm$ SD of data from three independent experiments. **, $P < 0.01$.

mutation was introduced into poMx1 to generate the poMx1 (M528D). The results showed that poMx1 (M528D) does not appear as a single monomer but undermined lower and higher oligomers. Mx-associated GTPase activity was detected in cells transfected with the constructs indicated in Fig. 1C, and except for poMx1 (K83A), all the poMx1 mutants exhibited strong GTPase activities. These results are in agreement with those of previous studies (30).

Mx proteins inhibit CSFV replication. Our previous work demonstrated that poMx1 can inhibit CSFV replication *in vitro* and *in vivo* (25, 26). Here, we asked if poMx1 (mutants), poMx2 (WT), huMxA (WT), or mmMx1 (WT) could inhibit CSFV replication. PK-15 cells were transfected with pcDNA-poMx1-HA (WT and mutants), pcDNA-poMx2-HA, pcDNA-huMxA-HA, pcDNA-mmMx1-HA, or pcDNA3.0. Transfected cells were infected with CSFV Shimen strain at a multiplicity of infection (MOI) of 0.1. Viral RNA and protein levels and virus titers were determined by Western blotting, reverse transcription quantitative PCR (RT-qPCR), and 50% tissue culture infective dose ($TCID_{50}$). At 24 and 48 h postinfection (hpi), both RT-qPCR and $TCID_{50}$ results demonstrated that all WT Mx proteins and poMx1 mutants L618D and E646R inhibited CSFV replication. However, poMx1 mutants K83A, R409D, and ΔL4 did not interfere with CSFV replication to any greater extent than the vector-alone control (Fig. 2A and B). At 48 hpi, results of Western blotting of these samples harvested and probed for viral envelope glycoprotein (E2) further revealed that except for poMx1 mutants K83A, R409D, and ΔL4, all WT Mx proteins and poMx1 mutants L618D and E646R inhibited CSFV replication (Fig. 2B). In addition, inactive mmMx1 mutant K49A showed no anti-CSFV activity (Fig. 2C). Finally, the infected cells overexpressing the different Mx proteins were detected using confocal microscopy (as indicated in Fig. 2D), and infection rates were calculated (Fig. 2E). The results showed that the infection rates of cells overexpressing poMx1 WT or the L618D or E646R mutant, poMx2 (WT), huMxA (WT), and mmMx1 (WT) significantly decreased compared to those of cells overexpressing the poMx1 mutants K83A, R409D, and ΔL4 or the vector control and mock-infected cells. In summary, the poMx1 mutants L618D and E646R retain anti-CSFV activity equal to that of WT levels *in vitro* while poMx1 mutants K83A, R409D, and ΔL4 have completely lost anti-CSFV activity.

Porcine Mx depletion enhances CSFV replication. A series of specific small interfering RNA (siRNA) duplexes was used to silence the expression of endogenous

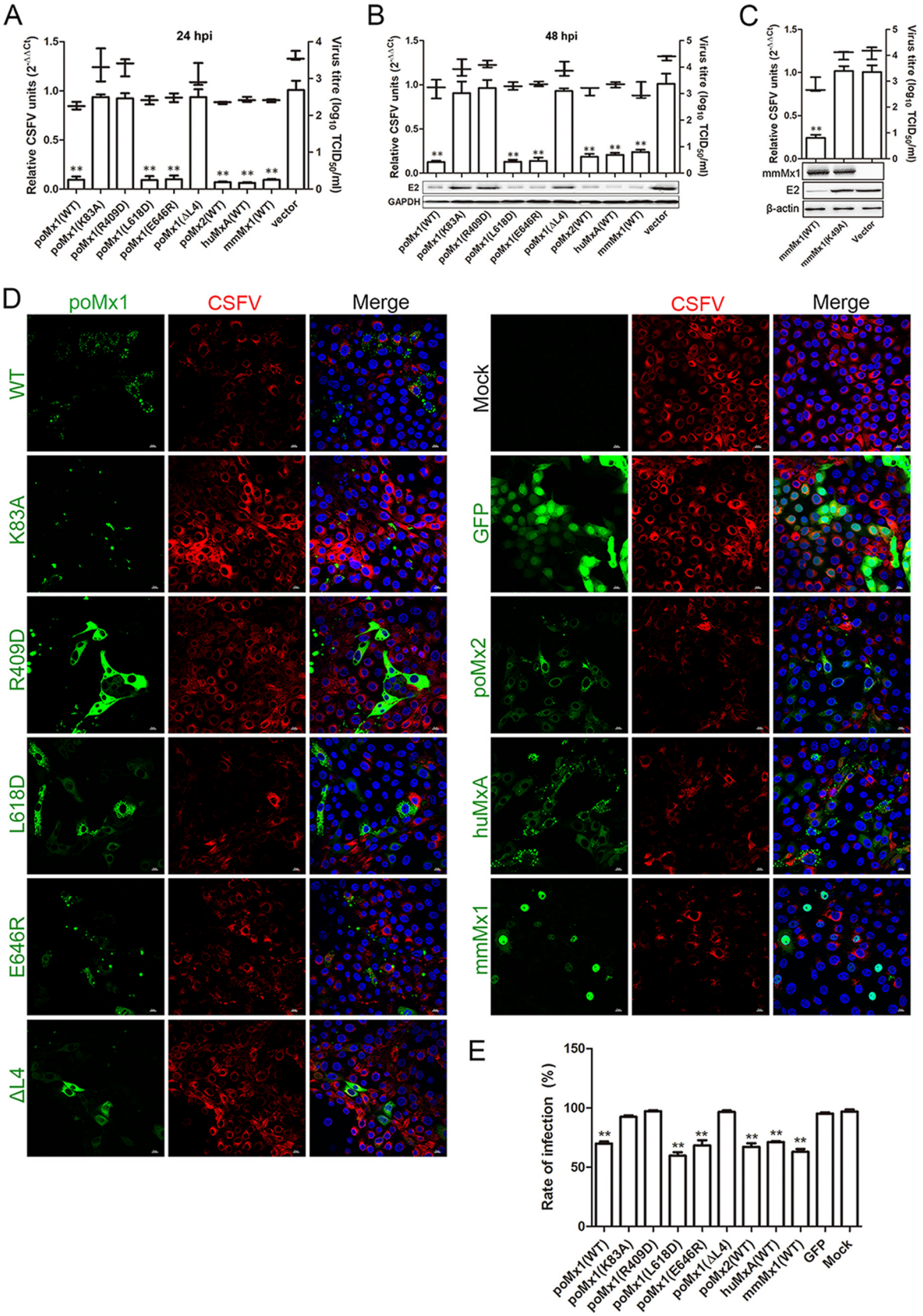

FIG 2 Antiviral effects of Mx proteins. PK-15 cells transfected with pcDNA-poMx1-HA (WT and mutants), pcDNA-poMx2-HA, pcDNA-huMxA-HA, pcDNA-mmMx1-HA (WT and K49A mutant), or pcDNA3.0 and infected with the CSFV Shimen strain (MOI of 0.1). (A) At 24 hpi, viral RNA

(Continued on next page)

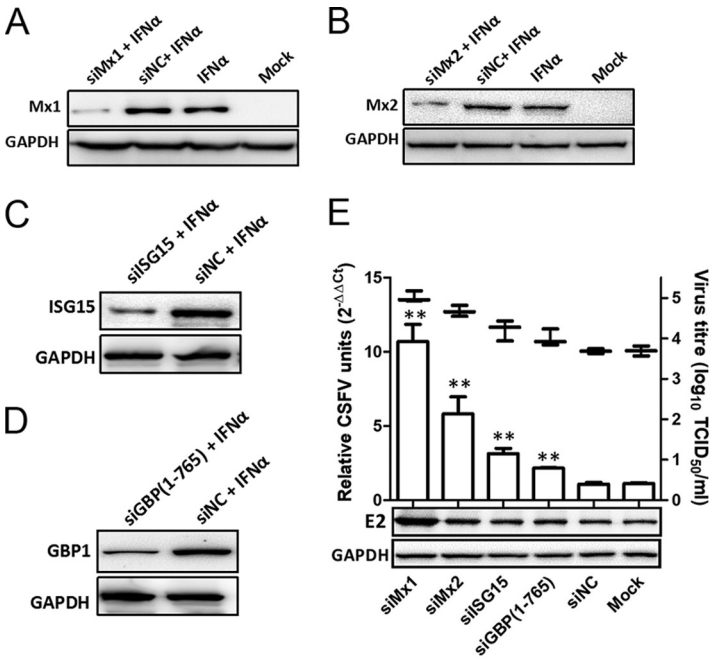

FIG 3 Porcine Mx depletion enhances CSFV replication. (A to D) Efficiency of siMx1, siMx2, $siGBP_{1-765}$, or siISG15 in PK-15 cells. Western blotting was performed on lysates from PK-15 cells treated with 100 nM siMx1, siMx2, $siGBP_{1-765}$, siISG15, or siNC for 12 h and then treated with 100 ng of huIFN-α for 36 h. poMx1, poMx2, GBP-1, ISG15, and GAPDH were detected using mouse monoclonal antibodies against poMx1, poMx2, GBP-1, ISG15, and GAPDH, respectively. (E) Effects of Mx1, Mx2, GBP-1_{1-765}, or ISG15 on CSFV replication. PK-15 cells pretreated with siRNAs were treated with 100 ng of huIFN-α for 36 h and then infected with CSFV at an MOI of 0.1 for 48 h. Viral RNA levels, virus titers, and viral E2 levels were determined by RT-qPCR, $TCID_{50}$, and Western blotting, respectively. Results are presented as the means $\pm$ SD of data from three independent experiments. **, $P < 0.01$.

poMx1 or poMx2, as well as that of IFN-stimulated gene 15 (ISG15) and guanylate binding protein 1 (GBP-1) as positive controls. These siRNAs resulted in efficient reduction of these four proteins (Fig. 3A to D). Subsequently, the replication efficiency of CSFV in cells transfected with these siRNAs was assessed using RT-qPCR, $TCID_{50}$, and Western blotting. RT-qPCR indicated that viral RNA copy numbers in infected cells transfected with an siRNA targeting Mx1 (siMx1), siMx2, siISG15, and an siRNA targeting residues 1 to 765 of GBP-1 ($siGBP_{1-765}$) were greater than those of mock transfected cells or cells transfected with a nontargeting control siRNA (siNC) (Fig. 3E). Intriguingly, viral RNA copies in siMx1- and siMx2-transfected cells were significantly increased over levels in siISG15- or $siGBP_{1-765}$-transfected cells, suggesting that porcine Mx proteins, especially poMx1, play an important role in innate immunity against CSFV. As expected, viral titers and Western blotting supported these results (Fig. 3E). Taken together, these results indicate that knockdown of endogenous poMx1 or poMx2 enhances CSFV replication, suggesting that porcine Mx proteins are critical cellular antiviral factors against CSFV infection.

Mx proteins are associated with the ER. Previous studies have demonstrated that Hook3, mannose-6-phosphate receptor, and Lamp-1, colocalize with huMxA (WT) in a distinct subcompartment of the smooth endoplasmic reticulum (ER) (31, 32). To test whether poMx1 proteins (WT and mutants) or poMx2 (WT) is also associated with the

FIG 2 Legend (Continued)
levels and virus titers were determined by RT-qPCR and $TCID_{50}$. (B) At 48 hpi, viral RNA levels, virus titers, and E2 protein levels in cell culture were determined by RT-qPCR, $TCID_{50}$, and Western blotting, respectively. (C) RT-qPCR, $TCID_{50}$, and Western blotting were performed to identify the antiviral activities of mmMx1 (WT and K49A mutant). In panels A to C, RT-qPCR results are represented on the left *y* axis, and $TCID_{50}$ results are represented on the right *y* axis. Finally, the infected cells overexpressing the different indicated Mx proteins were detected using confocal microscopy (D) and used to calculate infection rate (E). Results are presented as the means $\pm$ SD of data from three independent experiments. **, $P < 0.01$.

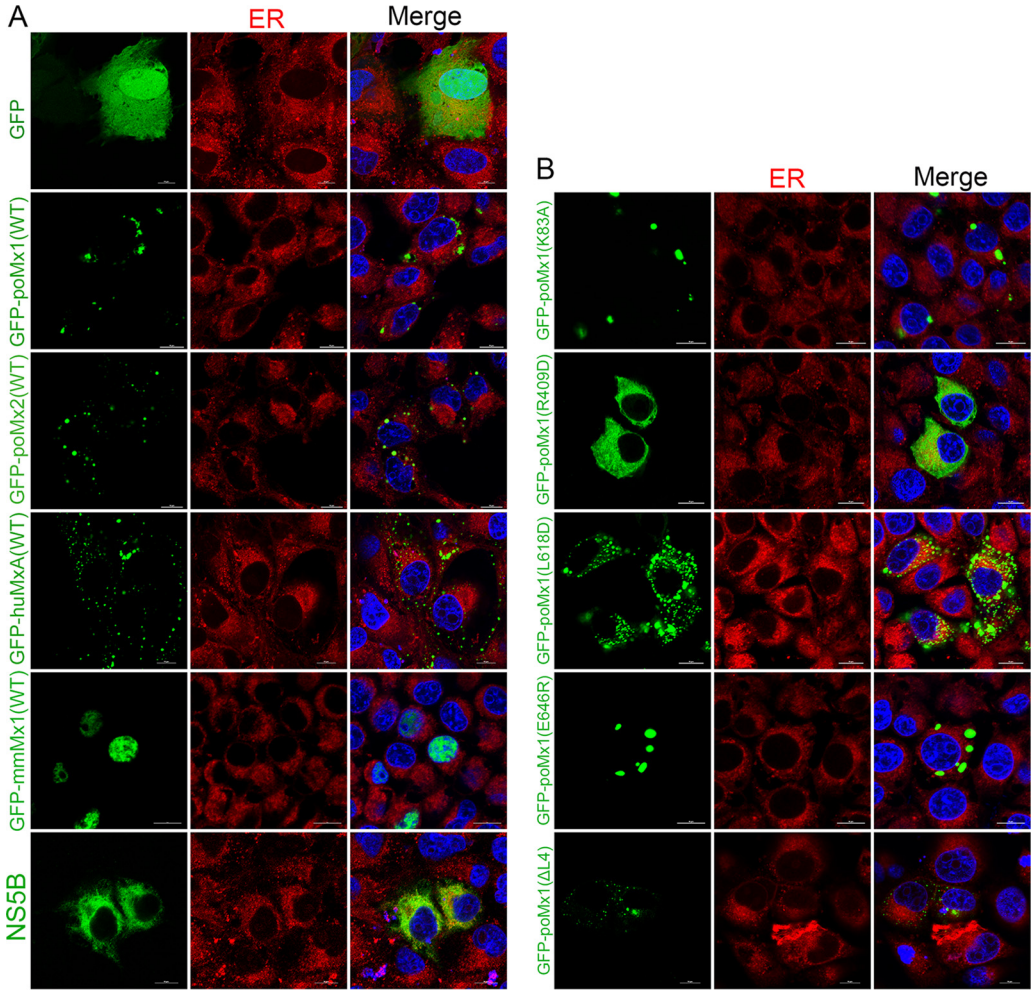

FIG 4 Mx proteins are associated with the endoplasmic reticulum (ER). (A and B) PK-15 cells were transfected with pEGFP-poMx1 (WT and mutants), pEGFP-poMx2, pEGFP-huMxA, pEGFP-mmMx1, pEGFP-C1, or pFLAG-NS5B. At 24 hpt, monolayers were stained with Alexa Fluor 568-labeled endoplasmic reticulum (1:1,000) for 30 min and then fixed and stained with DAPI. Bar, 10 μm.

ER, the subcellular locations of the proteins were determined using confocal microscopy. As anticipated, all the Mx proteins including the poMx1 mutants were associated with the ER (Fig. 4A and B), suggesting that the antiviral action of poMx1 or poMx2 against CSFV infection may happen in the ER. huMxA was used as a positive control, and mmMx1, known to locate in the nucleus, was a negative control. Our results are in agreement with previous reports (16). Furthermore, we transfected the construct encoding CSFV NS5B into PK-15 cells. Confocal microscopy indicated that it was also near the ER, which is also consistent with a previous report (33).

poMx1 targets CSFV NS5B. Experimental evidence for a physical interaction between poMx1 or poMx2 and CSFV is lacking. To address this, the interaction between poMx1 or poMx2 and CSFV was investigated using confocal microscopy, co-IP, and GST pulldown assays. PK-15 cells were cotransfected with pEGFP-poMx1 (where EGFP is enhanced green fluorescent protein) or pEGFP-poMx2 and pFLAG-Core, pFLAG-NS2, pFLAG-NS3, pFLAG-NS4B, pFLAG-NS5A, or pFLAG-NS5B and fixed at 24 h posttransfection (hpt). Confocal microscopy indicated colocalization of poMx1 (green) and NS5B (red) in the cytoplasm. There was no colocalization of poMx1 with the other expressed CSFV proteins (Fig. 5A and C). poMx2 did not colocalize with any of the expressed CSFV proteins (Fig. 5B and D). For co-IP, 293T cells were cotransfected with pcDNA-poMx1-HA or pcDNA-poMx2-HA and pFLAG-Core, pFLAG-NS2, pFLAG-NS3, pFLAG-NS4B, pFLAG-

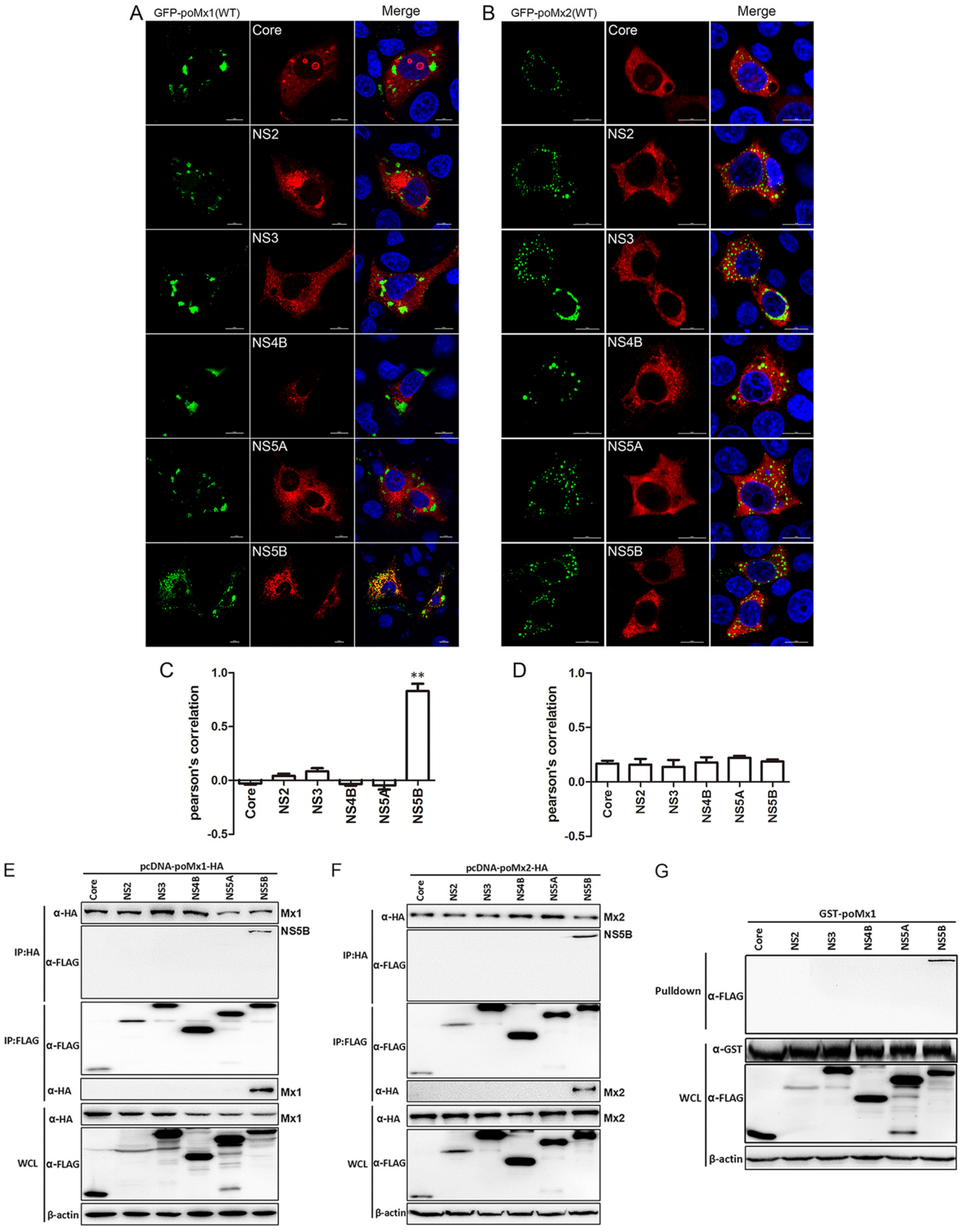

FIG 5 CSFV NS5B interacts with poMx1 but not poMx2. (A and B) PK-15 cells were cotransfected with pEGFP-poMx1 or pEGFP-poMx2 and pFLAG-Core, pFLAG-NS2, pFLAG-NS3, pFLAG-NS4B, pFLAG-NS5A, or pFLAG-NS5B. At 24 hpt, monolayers were fixed with 4% paraformaldehyde, permeabilized with 0.1%

(Continued on next page)

NS5A, or pFLAG-NS5B and then lysed at 48 hpt. Immunoprecipitation of HA and FLAG revealed that poMx1 and poMx2 efficiently coprecipitated with NS5B (Fig. 5E and F). To further test the interaction between poMx1 and NS5B, GST pulldown assays were performed. The results showed that GST-poMx1 interacted only with NS5B (Fig. 5G). These data strongly support our hypothesis that poMx1 inhibits viral replication by targeting CSFV NS5B, while poMx2 associates with NS5B, suggesting that the two poMx proteins inhibit CSFV replication using different pathways.

GTPase activity and stable oligomerization of poMx1 are critical for interacting with NS5B. Since poMx1 inhibits CSFV replication by interacting with NS5B, we cotransfected PK-15 cells with pFLAG-NS5B and pEGFP-poMx1 (WT and mutants), pEGFP-poMx2, pEGFP-huMxA, or pEGFP-mmMx1 and fixed cells at 24 hpt for confocal microscopy. The results indicated colocalization of NS5B and poMx1 WT and mutants L618D and E646R and huMxA (WT). There was no colocalization between NS5B and poMx2 (WT) or mmMx1 (WT), and as expected there was no colocalization between NS5B and GTPase-deficient poMx1 (K83A), oligomerization-disrupting poMx1 (R409D), and interaction-interfering poMx1 (ΔL4) (Fig. 6A and B).

293T cells were cotransfected with pcDNA-poMx1-HA (WT and mutants), pcDNA-poMx2-HA, pcDNA-huMxA-HA, or pcDNA-mmMx1-HA and pFLAG-NS5B. A co-IP assay was performed at 48 hpt, and the precipitating antibodies were anti-HA, anti-FLAG, or anti-NS5B antibody. poMx1 (WT), poMx1 (L618D), poMx1 (E646R), poMx2 (WT), and huMxA (WT) coprecipitated with FLAG-NS5B (Fig. 6C). That mmMx1 does not colocalize or co-IP with NS5B suggests that it inhibits CSFV replication via another mechanism.

Finally, PK-15 cells were transfected with the indicated (on the figures) constructs and then infected with CSFV (MOI of 0.1). At 48 hpi, the infected cells were fixed and probed with mouse anti-NS5B polyclonal antibody (produced in our lab) for determining colocalization of different Mx proteins and NS5B. Confocal microscopy showed similar results in the infected state and indicated colocalization of CSFV NS5B and poMx1 WT, L618D, or E646R or huMxA (WT) but not poMx1 K83A, R409D, or ΔL4, poMx2 (WT), or mmMx1 (WT) (Fig. 6D and E). GST pulldown showed that only poMx1 (WT), poMx1 (L618D), and poMx1 (E646R) interacted with NS5B (Fig. 6F).

PK-15 cells were cotransfected either with NS5B tagged with amino-terminal residues 1 to 173 of the Venus fluorescent protein (VN-NS5B) or with poMx1 tagged with Venus carboxyl-terminal residues 174 to 239 (VC-poMx1) (WT and mutants) and then lysed at 24 hpt for Western blotting with anti-poMx1 MAb (catalog number 79609; Abcam) or anti-NS5B polyclonal antibody (PAb) (Fig. 7B) or fixed at 16 hpt for confocal microscopy. The results of BiFC assays showed that VN-NS5B and poMx1 (WT), poMx1 (L618D), or poMx1 (E646R) produced positive BiFC signals (Fig. 7A and C). Taken together, these data demonstrate that poMx1 inhibits CSFV replication by targeting viral NS5B, as well as huMxA, and that GTPase activity and stable oligomerization of poMx1 are necessary for its interaction with NS5B and for its anti-CSFV activity.

To investigate whether poMx1 proteins undermine the RdRp activities of NS5B, we expressed and purified poMx1 proteins (WT and mutants) and NS5B proteins. Each protein was able to be immunoblotted with anti-His_6 tag monoclonal antibody, which was not found in the control (Fig. 8A to C). To evaluate the biological activity of CSFV NS5B, the RdRp activities of NS5B proteins were tested in the presence of increasing amounts of NS5B proteins (0, 50, 100, 150, 200, 250, and 300 ng) with the RNA templates under the conditions for RNA polymerization. Quantification of synthesized

FIG 5 Legend (Continued)

Triton X-100, reacted with anti-Flag MAb (1:1,000), and stained with DAPI. Bar, 10 μm. (C and D) The colocalization coefficients were expressed as Pearson's coefficient, measured for individual cells. (E and F) HEK293T cells were cotransfected with pHA-poMx1 or pHA-poMx2 and pFLAG-Core, pFLAG-NS2, pFLAG-NS3, pFLAG-NS4B, pFLAG-NS5A, or pFLAG-NS5B. At 48 hpt, cells were harvested and subjected to co-IP assay using mouse anti-Flag MAb (1:200) or mouse anti-HA MAb (1:200); the resulting complexes were subjected to Western blotting using rabbit anti-Flag MAb and rabbit anti-HA MAb. In addition, the whole-cell lysates (WCL) were analyzed for expression of HA, FLAG, and β-actin. (G) GST-poMx1 (WT and mutants) fusion proteins were expressed in *E. coli* BL21, purified with glutathione MagBeads, and incubated with FLAG-Core, FLAG-NS2, FLAG-NS3, FLAG-NS4B, FLAG-NS5A, or FLAG-NS5B. The resulting complexes were subjected to Western blotting using mouse anti-GST MAb and mouse anti-Flag MAb. In addition, the whole-cell lysates (WCL) were assayed for expression of GST, FLAG, and β-actin. **, $P < 0.01$.

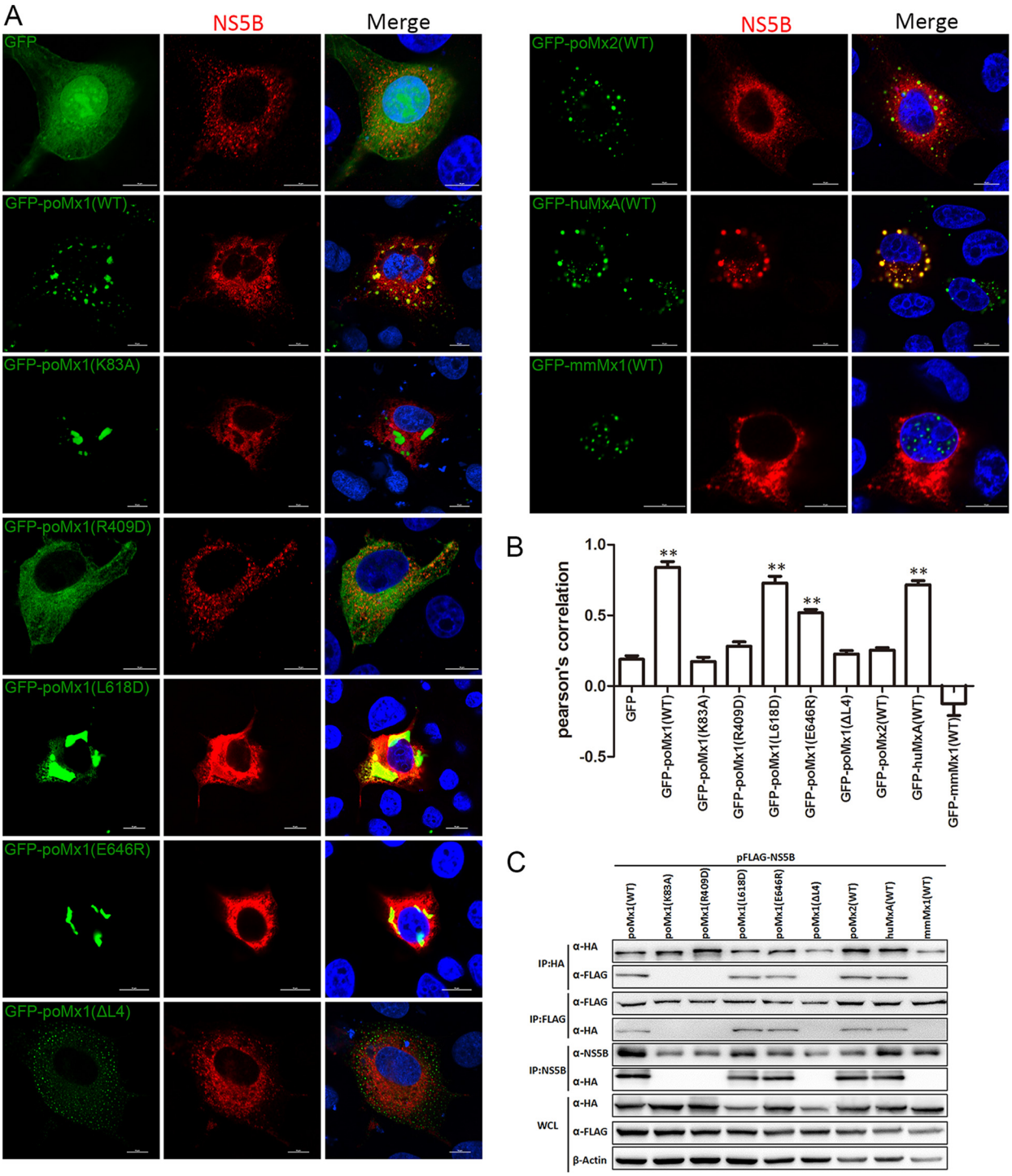

FIG 6 Interaction between NS5B and poMx1 variants, huMxA, and mmMx1. (A) The colocalization of NS5B and poMx1 variants, poMx2, huMxA, and mmMx1. PK-15 cells were cotransfected with pFLAG-NS5B and pEGFP-poMx1 (WT and mutants), pEGFP-poMx2 (WT), pEGFP-huMxA (WT), or pEGFP-mmMx1 (WT) (2 μg each). At 24 hpt, monolayers were fixed with 4% paraformaldehyde, permeabilized with 0.1% Triton X-100, reacted with anti-Flag MAb (1:1000), and stained with DAPI. Bar, 10 μm. (B) The colocalization coefficients were expressed as Pearson's coefficient, measured for individual cells. (C) HEK293T cells were cotransfected with pFLAG-NS5B and pEGFP-poMx1 (WT and mutants), poMx2 (WT), huMxA (WT), or mmMx1 (WT). At 48 hpt, cells were harvested and subjected to a co-IP assay using mouse anti-Flag MAb (1:200), mouse anti-HA MAb (1:200), or mouse anti-NS5B PAb (1:100). The resulting complexes were subjected to Western blotting using rabbit anti-Flag MAb, rabbit anti-HA MAb, and mouse anti-NS5B PAb. The whole-cell lysates (WCL) were also assayed for expression of HA, FLAG, and β-actin. (D) PK-15 cells were transfected with the indicated constructs and then infected with CSFV (MOI of 0.1). At 48 hpi, cells were fixed and probed with mouse anti-NS5B PAb (1:100) for determining colocalization of different Mx proteins and NS5B using confocal microscopy. Bar, 10 μm. (E) The colocalization coefficients were expressed as Pearson's coefficient, measured for individual cells. (F) GST or the GST-poMx1 (WT and mutants) fusion proteins were expressed in *E. coli* BL21, purified with glutathione MagBeads, and then incubated with the FLAG-NS5B protein. The resulting complexes were subjected to Western blotting using mouse anti-GST MAb and mouse anti-Flag MAb. In addition, the whole-cell lysates (WCL) were assayed for expression of GST, FLAG, and β-actin. **, $P < 0.01$.

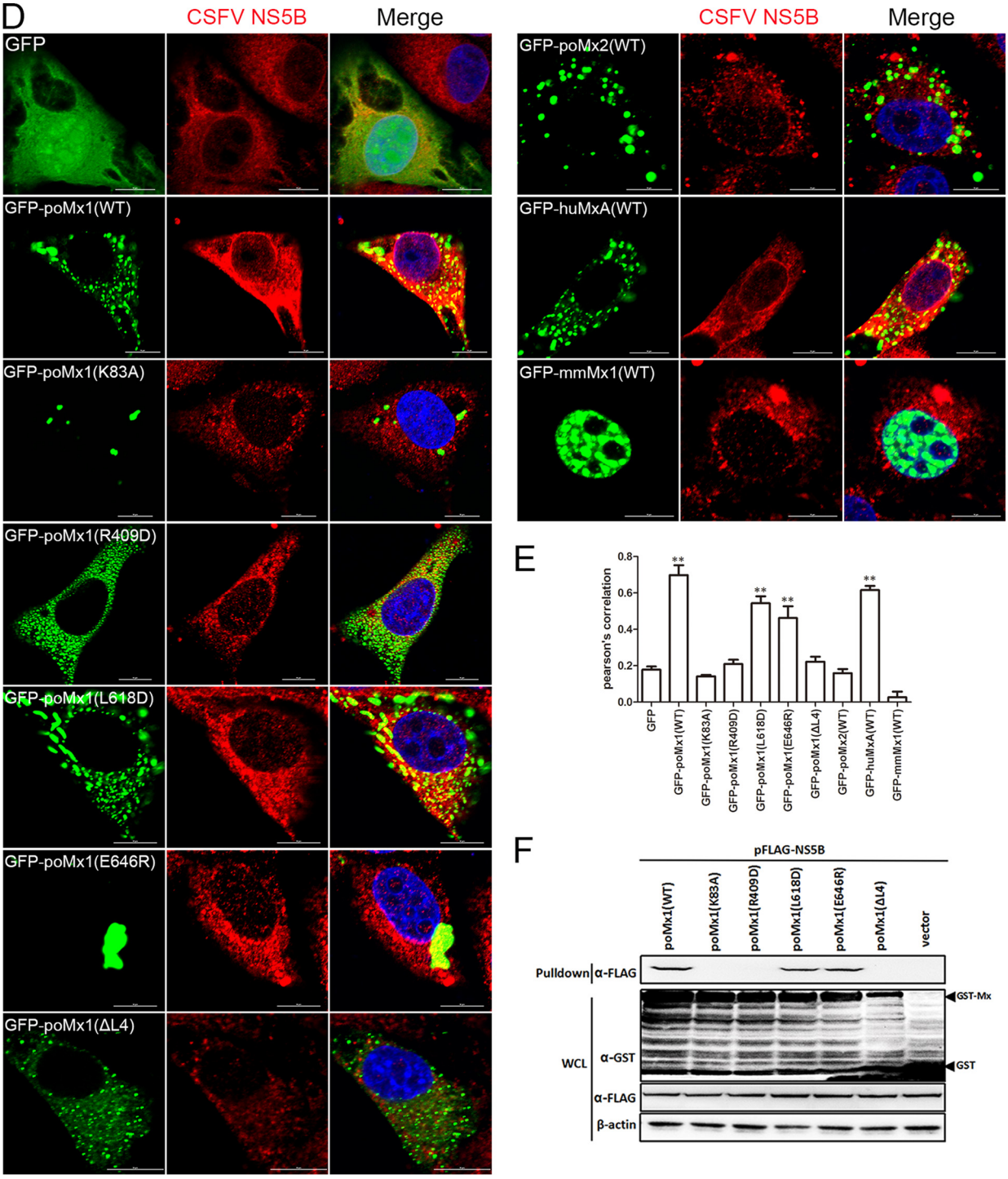

FIG 6 (Continued)

RNA was determined by real-time RT-PCR. The results showed that newly synthesized RNA products were detected (Fig. 8A), indicating that the purified NS5B protein was able to catalyze RNA synthesis and that 100 ng was the most effective amount. For the influence of poMx1 on RdRp activities of NS5B, RNA templates were incubated with 100 ng of NS5B proteins and increasing amounts of poMx1 proteins (WT) (0, 50, 100, 150, 200, 250, 300 ng) under the same conditions. The results showed that poMx1 undermined the RdRp activity of NS5B proteins, and the

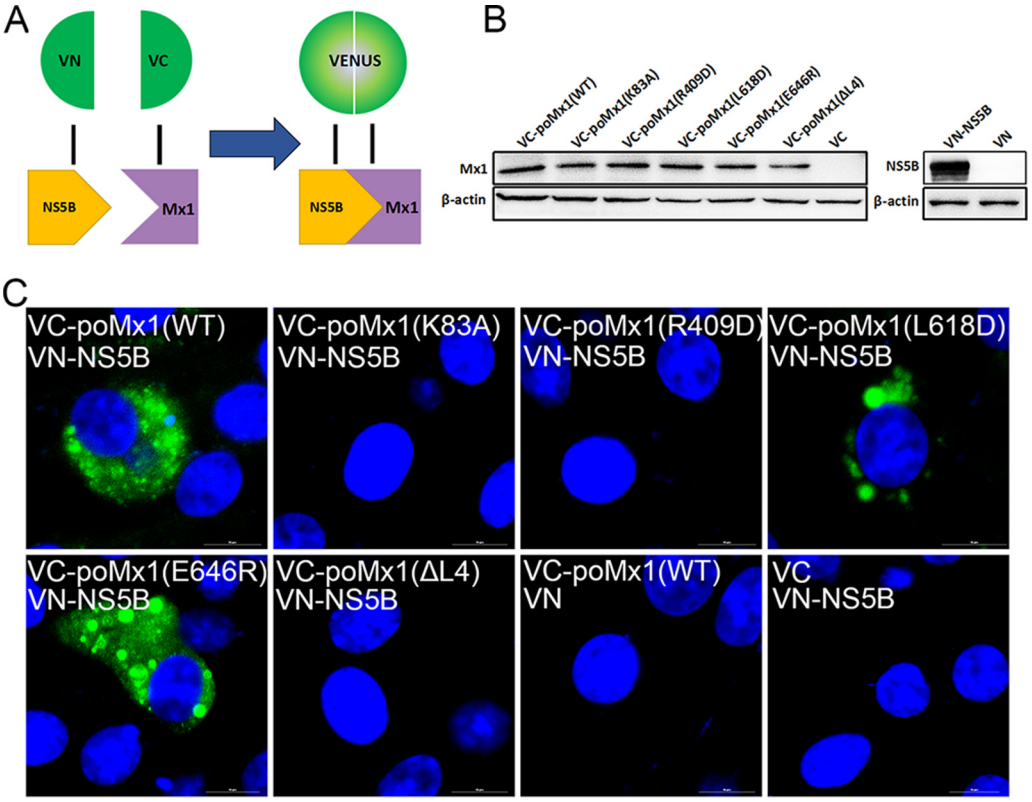

FIG 7 BiFC assay of NS5B and poMx1 (WT and mutants) interactions. (A) Principle of BiFC system. (B) In this study, Western blotting was performed of lysates from cells transfected with VC-poMx1 (WT or mutants) or VN-NS5B probed with anti-poMx1 MAb or anti-NS5B PAb and anti-β-actin MAb. (C) The fluorescence visualized in the living cells. Mx (WT or mutants) and NS5B were fused to the N- and C-terminal fragments of a fluorescent protein, respectively. When there are two proteins associated, the two fragments are brought together to facilitate reconstruction of the fluorescent protein, reproducing emission of fluorescence under excitation.

reduction in activity was in agreement with the increasing amount of poMx1 (Fig. 8B). When 100 ng of NS5B protein was incubated with 100 ng of poMx1 protein (WT or mutant) for RdRp activity assays, the results demonstrated that poMx1 WT, L618D, or E646R was able to undermine the RdRp activity of NS5B although other poMx1 mutants did not (Fig. 8C).

Mx proteins do not affect functional endosomes. To test whether expression of Mx proteins influences the localization or the function of membrane compartments, we analyzed Mx-overexpressing cells for endocytosis. Our results showed that uptake of transferrin (Tfn) occurred normally in Mx-expressing cells (Fig. 9A). There was no difference in Tfn signal intensities among any Mx proteins (Fig. 9B).

Rab proteins play major roles in endocytic vesicle trafficking (34). Of these, Rab5 is involved in the life cycles of multiple viruses in the family *Flaviviridae* and is an important factor in the process of CSFV endocytosis (35). Here, we tested whether overexpression of Mx protein affects CSFV endocytosis. PK-15 cells transfected with the indicated (on the figures) Mx constructs were infected with CSFV and then fixed after 30 min for confocal microscopy. The results showed that no Mx protein colocalized with Rab5 in infected cells (Fig. 10A and B), suggesting that Mx protein does not hijack early endosomes to affect virus endocytosis and that Mx expression does not lead to a disturbance of the endosomal compartment. Further, there was no difference in viral RNA copy numbers and Rab5 protein levels between the infected cells overexpressing the indicated (on the figures) Mx constructs and control construct (Fig. 10C). Taken together, these results show that Mx overexpression had no effect on CSFV endocytosis mediated by Rab5.

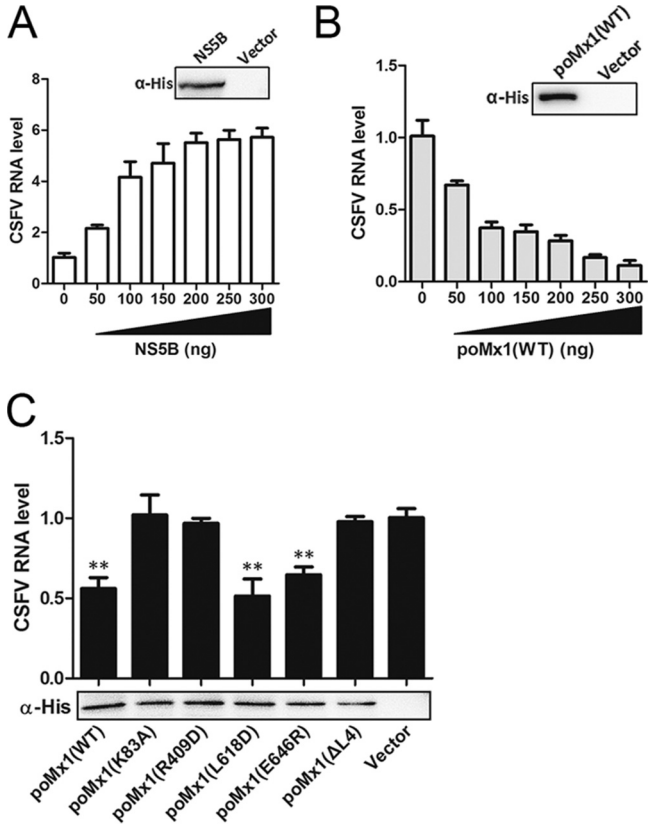

FIG 8 poMx1 proteins undermine the RdRp activity of NS5B proteins. RdRp assays were performed as follows: with increasing amounts of NS5B proteins (0, 50, 100, 150, 200, 250, and 300 ng) (A); with 100 ng of NS5B proteins and increasing amounts of poMx1 proteins (WT) (0, 50, 100, 150, 200, 250, or 300 ng) (B); with 100 ng of NS5B proteins and 100 ng of poMx1 proteins (WT and mutant) with the RNA templates (C). Quantification of synthesized RNA was determined using RT-qPCR as described in Materials and Methods. The results showed that newly synthesized RNA products were detected. Results are presented as the means ± SD of data from three independent experiments. **, $P < 0.01$.

DISCUSSION

Earlier work has shown that huMxA can inhibit CSFV replication (24), and our previous studies have demonstrated that overexpressed EGFP-poMx1 and protein transduction domain (PTD)-poMx1 fusion proteins inhibit CSFV replication in PK-15 cells in a dose-dependent manner (26). These observations suggest that huMxA and poMx1 may offer novel therapies against CSFV infection. In this study, we used poMx1 mutants to look at the connection between the structure and anti-CSFV activity of poMx1.

Previous studies have shown that human and mouse Mx proteins restrict the replication of FLUAV by recognizing the nucleocapsid protein (NP) (36, 37). The FLUAV polymerase subunit PB2 which is associated with NP may serve as an additional target. In our study, we clarified the mechanism by which poMx1 inhibits CSFV replication by targeting its nonstructural protein 5B (NS5B) for mutational analysis. CSFV has a single-stranded positive-sense RNA genome, coding for one polyprotein that is processed into mature proteins by cellular and viral proteases (Npro, C, Erns, E1, E2, p7, NS2, NS3, NS4A, NS4B, NS5A, and NS5B) (38). CSFV is a member of the genus *Pestivirus* (family *Flaviviridae*) along with BVDV-1, BVDV-2, and border disease virus (BDV) (39). Hepatitis C virus (HCV), the major cause of transfusion-associated hepatitis, also belongs to this family (40). It is well known that NS5B is the viral RNA-dependent RNA polymerase responsible for transcription and replication of the viral genome, and NS5B has been shown to function as part of a larger, membrane-associated replication complex (41, 42). Previous studies have shown that inhibitors such as compound VP32947, compound 1457, and BPIP (5-[(4-bromophenyl)methyl]-2-phenyl-5*H*-imidazo[4,5-*c*]pyridine) inhibit pestivirus (CSFV or BVDV) replication by targeting NS5B

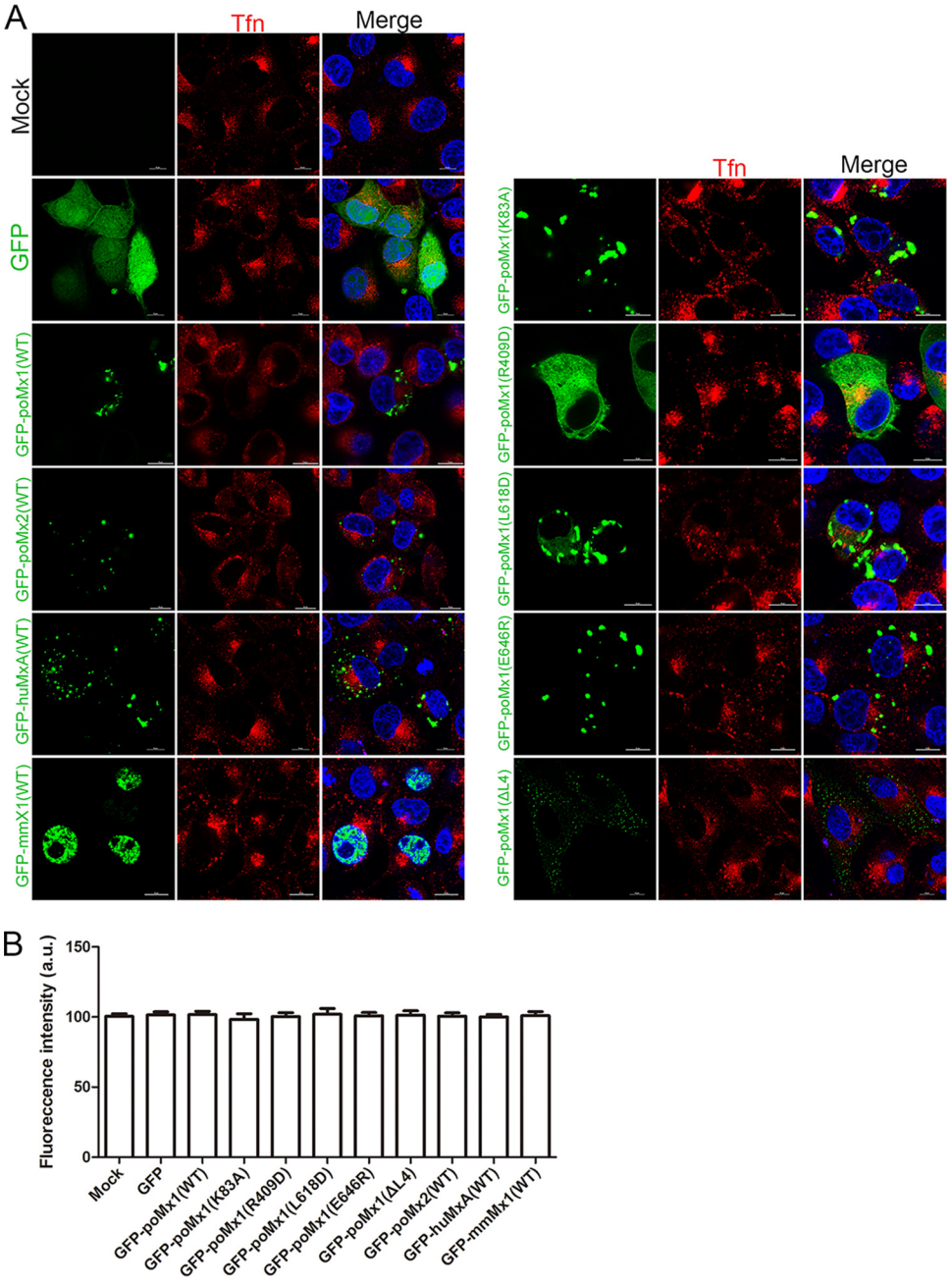

FIG 9 Mx proteins do not affect cell endocytosis. (A) Mx proteins do not colocalize with Tfn. PK-15 cells were transfected with pEGFP-poMx1 (WT or mutants), pEGFP-poMx2 (WT), pEGFP-huMxA (WT), pEGFP-mmMx1 (WT), or pEGFP-C1. At 24 hpt, cells were incubated with 10 μg/ml Alexa Fluor 568-labeled Tfn for 30 min at 4°C and then transferred to 37°C for 30 min. Cells were fixed and stained with DAPI. Bar, 10 μm. (B) Total fluorescence intensity per cell was calculated using Nikon NIS-Elements AR, version 4.5, analysis software. Tfn uptake is represented as means ± SD of integrated fluorescence intensities from two independent experiments. au, arbitrary units.

(43–45). A similar interaction between VP32947 and HCV NS5B has also been observed (46). Therefore, NS5B of the *Flaviviridae* is an important target for inhibitors.

GTPase activity is necessary for MxA to act against RNA viruses (47, 48). The GTPase domain is the most conserved region in Mx proteins and other members of the dynamin family of large GTPases. Mutations in the GTP binding element of MxA invariably cause a loss of antiviral activity, indicating that GTP binding and/or hydrolysis is critical for function. Additionally, the C terminus is required for GTPase activity. Previous studies have shown that the mutation K83A in huMxA renders the protein

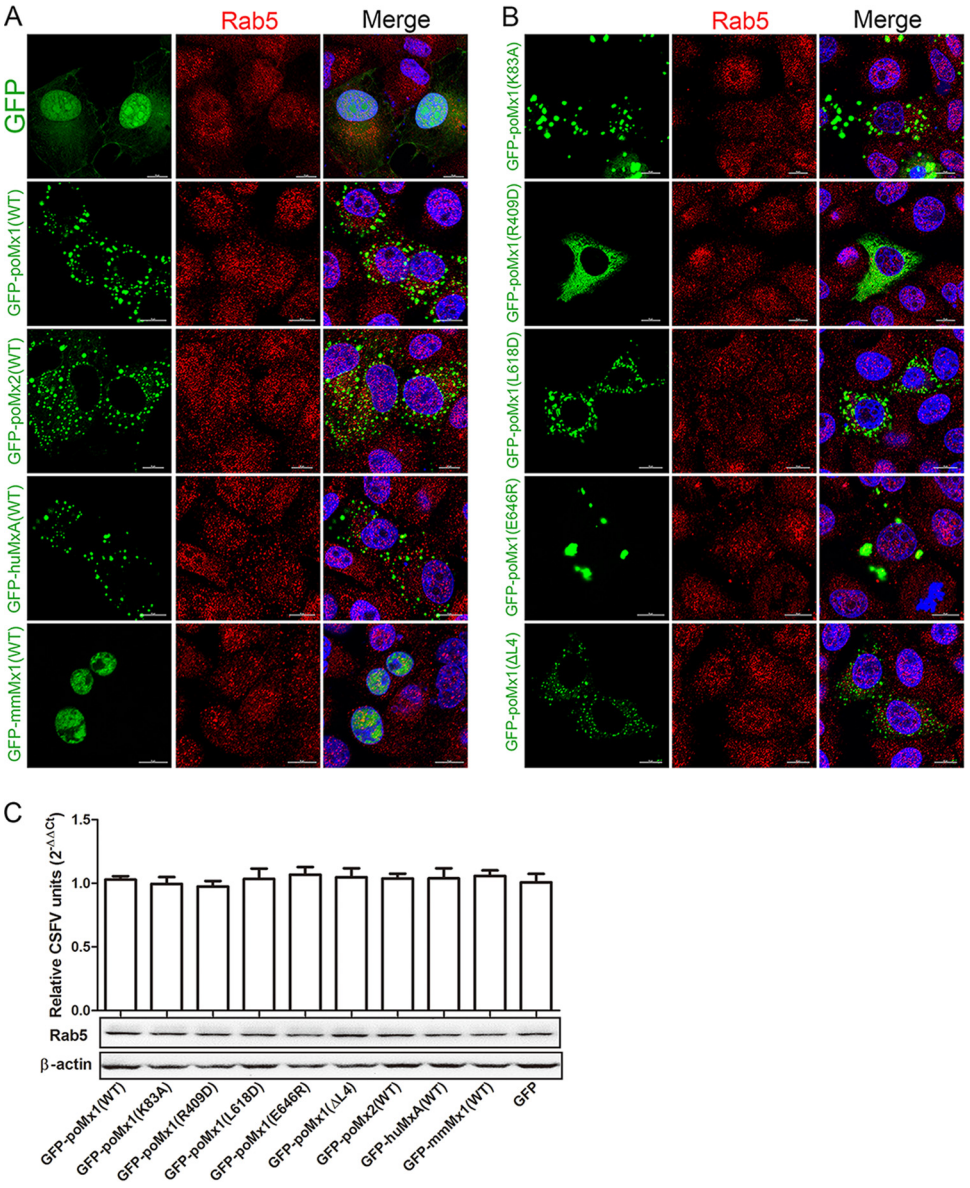

FIG 10 Mx proteins have no effect on endosomal trafficking of CSFV. (A and B) Mx proteins have no effect on Rab5 distribution in the infected cells. PK-15 cells were transfected with the indicated constructs for 48 h and then infected with CSFV (MOI of 5) at 4°C for 1 h and then shifted to 37°C for 30 min. Cells were fixed, reacted with rabbit anti-Rab5 antibody, and stained with DAPI. Bar, 10 μm. (C) Viral RNA copy number was determined by RT-qPCR, and Rab5 protein level was determined by Western blotting.

unable to inhibit the replication of viruses, such as VSV, influenza A virus (49), and La Crosse virus (50), demonstrating that its GTPase activity is necessary for antiviral function. Although we previously showed that poMx1 can inhibit CSFV replication, it was unclear whether GTPase activity of poMx1 is required for this inhibition. To address this, we modeled the huMxA mutants and constructed a poMx1 (K83A) mutant that no longer contained a normal GTPase consensus element. We tested its GTPase activity and antiviral activity *in vitro*. As expected, we observed that all mutants exhibited an antiviral effect except poMx1 (K83A), suggesting the necessity of GTPase for the anti-CSFV effect of poMx1.

Gao et al. proposed that a mutation in the surface-exposed Arg-408 (409 in poMx1) in helix α1c in interface 3 of huMxA promoted disruption of tetramers and the formation of stable dimers, resulting in the loss of anti-FLUAV effects (9).We observed

similar results with poMx1 (R409D); it does not form stable tetramer or dimers but is in a mixed state of tetramers, dimers, and monomers, suggesting that there is no stable binding between poMx1 (R409D) and the RNA polymerase of CSFV, resulting in a loss anti-CSFV activity. Gao et al. also introduced L617D (L618D in poMx1) in stalk interface 1 of huMxA to disrupt tetramers into dimers (9), but with GTPase, which was verified by Nigg and Pavlovic, the mutant huMxA (L617D) still harbors antiviral activity against FLUAV (11). The huMxA stalk contains a 40-amino-acid loop 4 (residues 533 to 572) that is located at a position equivalent to the PH domain of dynamin and serves as a docking site for membranes or viral targets (48, 51). We found that deleting the L4 loop in poMx1 resulted in loss of interaction with NS5B and the loss of anti-CSFV activity. We demonstrated that the anti-CSFV mechanism of huMxA is the same as that of poMx1. The anti-CSFV activities of both proteins depend on targeting the RNA polymerase of CSFV. In addition, previous studies have shown that huMxA (E645R), which differs from WT poMx1 by a single amino acid substitution near the C terminus, can inhibit the replication of influenza virus and *Thogotovirus* but is inactive against VSV and La Crosse virus (52, 53). In our study, poMx1 (E646R) retained anti-CSFV activity. This mutant was able to target NS5B.

In Landrace pigs the Mx2 protein can inhibit the multiplication of influenza virus (54, 55). However, little is known about the antiviral mechanism of poMx2 against CSFV. We found that poMx2 localizes to the cytoplasm, yet there is no colocalization with NS5B. The proteins did interact in co-IP, so we speculate that there is an indirect interaction between them. In future studies we will investigate the details of the interaction between poMx2 and NS5B and illustrate how poMx2 inhibits CSFV. mmMx1 was reported to inhibit FLUAV by specifically blocking viral mRNA synthesis that is catalyzed in the nucleus by the RNA polymerase residing in the incoming viral nucleocapsid (primary transcription). We have also found inhibition of CSFV by mmMx1 but not by mmMx1 (K49A). However, there is no colocalization or interaction between mmMx1 and the RNA polymerase of CSFV, suggesting that mmMx1 uses a yet-to-be identified mechanism to inhibit CSFV replication.

In conclusion, we have demonstrated that poMx1 (WT) targets NS5B, thereby inhibiting CSFV replication; poMx1 mutations L618D and E646R do not interfere with NS5B targeting and retain anti-CSFV activity. poMx1 mutations that do interfere with NS5B interaction, K83A, R409D, and ΔL4, do not retain any anti-CSFV activity. huMxA (WT) also has anti-CSFV activity and targets NS5B. poMx2 (WT) and mmMx1 (WT) inhibit CSFV replication although the mechanism is yet unknown.

MATERIALS AND METHODS

Cells, viruses, and interferon. Porcine kidney (PK-15) cells and human embryonic kidney (HEK293T) cells were cultured in Dulbecco's modified Eagle's medium (DMEM; Gibco, Invitrogen, Carlsbad, CA, USA) containing 10% fetal bovine serum (FBS; Gibco), 0.2% $NaHCO_3$, 100 μg/ml streptomycin, and 100 IU/ml penicillin (Gibco) at 37°C with 5% CO_2. The virulent CSFV Shimen strain (GenBank accession number AF092448) was obtained from the National Institute of Veterinary Drug Control (Beijing, China). Human interferon alpha-1b (huIFN-α) (29) was purchased from Shenzhen Kexing Biotech Co., Ltd. (China).

Plasmid construction and cell transfection. pcDNA3.0-poMx1-HA, pcDNA3.0-poMx2-HA, pEGFP-poMx1, and pEGFP-poMx2 have been described previously (26, 29). The human *MxA* gene (UniProt ID P20591) and mouse *Mx1* gene (UniProt ID P09922), which were kindly provided by Song Gao (Sun Yat-sen University Cancer Center, Guangzhou, China), were cloned into pcDNA3.0 fused to an HA tag or pEGFP-C1, creating pcDNA3.0-huMxA-HA, pcDNA3.0-mmMx1-HA, pEGFP-huMxA, or pEGFP-mmMx1. The poMx1 mutants poMx1 (K83A), poMx1 (R409D), poMx1 (L618D), poMx1 (E646R), and poMx1 (ΔL4) (deletion of residues 534 to 573) and the mutant mmMx1 (K49A) (11) were constructed by directed mutagenesis (Wuhan GeneCreate Biological Engineering Co., Ltd., China) based on pcDNA3.0-poMx1-HA. The wild-type and mutated poMx1 proteins were also cloned into pGEX-4T-1, pColdI, and VC. The core protein, NS2, NS3, NS4B, NS5A, or NS5B gene of CSFV was cloned into the p3×FLAG-CMV-7.1 vector to generate pFLAG-Core, pFLAG-NS2, pFLAG-NS3, pFLAG-NS4B, pFLAG-NS5A, or pFLAG-NS5B. NS5B was also cloned into VN and pColdI. The primers for amplification are listed in Table 1. All plasmids were confirmed by DNA sequencing. HEK293T or PK-15 cells were transfected with plasmids (2.5 μg each) using Lipofectamine 3000 (Invitrogen) in six-well plates according to the manufacturer's instructions. At 6 h posttransfection (hpt), fresh DMEM containing 2% FBS replaced the transfection mixture, and cells were incubated for an additional 48 h.

RNA interference. Two specific siRNAs targeting different regions of the *Mx1* and *Mx2* genes (sc-45260 and sc61110, respectively) and a nontargeting control siRNA ([siNC] sc-37007) were purchased

TABLE 1 The primers used in this study

Primer[a]	Sequence(5′–3′)	Use
pcDNA3.0-huMxA-F	TGACGAATTCACCATGGTTGTTTCCGAAGTGGA	Amplification of huMxA
pcDNA3.0-huMxA-R	TGACCTCGAGTTAAGCGTAGTCTGGGACGTCGTATGGGTAACCGGGGAA CTGGGCAAG	
pcDNA3.0-mmMx1-F	TGACGAATTCACCATGGATTCTGTGAATAATCTGTGC	Amplification of mmMx1
pcDNA3.0-mmMx1-R	TGACCTCGAGTTAAGCGTAGTCTGGGACGTCGTATGGGTAATCGGAGAA TTTGGCAAGCT	
pFLAG-CMVTM-7.1-Core-F	TGACGGTACCAATGTCTGATGATGGCGCAAGTGG	Amplification of core protein
pFLAG-CMVTM-7.1-Core-R	TGACGGATCCTTAGGCTTCAACTGGTTGATACAA	
pFLAG-CMVTM-7.1-NS2-F	TGACGAATTCAATGAGCGGGGTTGCCAAGGG	Amplification of NS2
pFLAG-CMVTM-7.1-NS2-R	TGACGGATCCTTATCTAAGCACCCAGCCAAG	
pFLAG-CMVTM-7.1-NS3-F	TGACGGTACCAATGGGGCCTGCCGTTTGCAAG	Amplification of NS3
pFLAG-CMVTM-7.1-NS3-R	TGACTCTAGATTATAGACCAACTACTTGTTTTAGTGCT	
pFLAG-CMVTM-7.1-NS4B-F	TGACGGTACCAATGGCTCAGGGGGATGTGCAG	Amplification of NS4B
pFLAG-CMVTM-7.1-NS4B-R	TGACGGATCCTTATAGCTGGCGGATCTTTCC	
pFLAG-CMVTM-7.1-NS5A-F	TGACGGTACCAATGTCAAGTAATTACATTCTAGAGCTCC	Amplification of NS5A
pFLAG-CMVTM-7.1-NS5A-R	TGACGGATCCTTACAGTTTCATAGAATACACTTTTGCA	
pFLAG-CMVTM-7.1-NS5B-F	TGACGAATTCAATGAGTAATTGGGTGATGCAAGAAG	Amplification of NS5B
pFLAG-CMVTM-7.1-NS5B-R	TGACGGATCCTTATACCCCTCTCCCTATCAGG	
pGEX-4T-1-poMx1-F	TGACGGATCCATGGTTTATTCCAACTGTGAAAG	Amplification of poMx1 for pulldown
pGEX-4T-1-poMx1-R	TGACCTCGAGTCAGCCTGGGAACTTGGCGA	
VC-poMx1-F	TGACGAATTCATGGTTTATTCCAACTGTGAAAGT	Amplification of poMx1 for BiFC
VC-poMx1-R	TGACCTCGAGGCCTGGGAACTTGGCGAGC	
VN-NS5B-F	TGACGAATTCATGAGTAATTGGGTGATGCAAGAAG	Amplification of NS5B for BiFC
VN-NS5B-R	TGACCTCGAGTACCCCTCTCCCTATCAGGG	
pCold1-poMx1-F	TGACCTCGAGATGGTTTATTCCAACTGTGAAAGTA	Amplification of poMx1 for RdRp
pCold1-poMx1-R	TGACGAATTCTCAGCCTGGGAACTTGG	
pCold1-NS5B-F	TGACCTCGAGAGTAATTGGGTGATGCAAGAAGA	Amplification of NS5B for RdRp
pCold1-NS5B-R	TGACGAATTCTACCCCTCTCCCTATCAGGG	
Q-CSFV-5′ UTR-F	GAACTGGGCTAGCCATG	qRT-PCR for detection of CSFV
Q-CSFV-5′ UTR-R	ACTGTCCTGTACTCAGGAC	
Q-GAPDH-F	GAAGGTCGGAGTGAACGGATTT	qRT-PCR for detection of GAPDH
Q-GAPDH-R	TGGGTGGAATCATACTGGAACA	

[a]F, forward; R, reverse; UTR, untranslated region.

from Santa Cruz Biotechnology, Inc.; ISG15 and GBP-1 genes were commercially synthesized by GenePharma (Shanghai, China). siRNA duplexes used in the study are listed in Table 2. PK-15 cells were seeded in six-well plates at 2.5×10^5 cells/well and then transfected with 100 nM siRNA using Lipofectamine 3000 according to the manufacturer's instructions. After 6 h, cell medium was replaced with fresh DMEM containing 2% FBS, and cells were incubated at 37°C. At 24 h posttransfection, the medium was aspirated and replaced with fresh complete medium containing 200 ng/ml huIFN-α; plates were incubated for another 48 h or infected with CSFV at an MOI of 0.1 and incubated for an additional 48 h. Cells were then collected for further analysis.

Western blotting. Cells were washed three times with cold phosphate-buffered saline (PBS) and lysed in cold lysis buffer (1% Triton X-100, 1 mM phenylmethylsulfonyl difluoride [PMSF] in PBS) for 30 min. Lysates were clarified by centrifugation at 12,000 $\times$ *g* for 10 min. Proteins in the lysates were separated by SDS-PAGE, transferred to nitrocellulose membranes, and then probed with the antibodies indicated in the figure legends. Glyceraldehyde-3-phosphate dehydrogenase (GAPDH) or β-actin was used as a loading control.

RT-qPCR. Total RNA was extracted from the infected PK-15 cells using TRIzol reagent (Invitrogen, USA), and viral RNA was measured using RT-qPCR as described previously (26). Data are presented as $2^{-\Delta\Delta CT}$ (where C_T is threshold cycle) from quadruplicate samples (56).

Virus titration. The transfected PK-15 cells were infected with the CSFV Shimen strain for 1 h. At 24 or 48 h postinfection (hpi), cells were lysed by three freeze-thaw cycles. Virus yields were determined as described previously (26). Data are presented as $TCID_{50}$s from quadruplicate samples.

Confocal fluorescence microscopy. PK-15 cells were grown on glass coverslips to 60% confluence. Cells were transfected with 2 μg of plasmid (for cotransfections, 2 μg of each plasmid was used) for 24 h at 37°C. Cells were then either (i) fixed with 4% paraformaldehyde in PBS, permeabilized with 0.1% Triton X-100, reacted with the appropriate antibody or reagent, and stained with

TABLE 2 siRNA duplexes used in this study

Primer	Sequence (5′–3′)	Use
siISG15	CUAUGUGCACCGUGUAUAUTT	ISG15 interference RNA
$siGBP_{1-765}$	GGACUCAGAAUUUGUGCAATT	GBP-1 interference RNA

4′,6′-diamidino-2-phenylindole (DAPI) or (ii) infected with the CSFV Shimen strain at an MOI of 0.1. After 48 h these cells were processed for confocal microscopy as described above. Antibodies used in this study were rabbit anti-Rab5 (ab18211; Abcam), mouse anti-CSFV E2 (WH303), and mouse anti-Flag MAb (F1804; Sigma-Aldrich). Other reactants were Alexa Fluor 568 (AF568)-labeled endoplasmic reticulum (702508; Life Technologies) and Alexa Fluor 568-labeled transferrin (1446005; Life Technologies). The colocalization coefficients were calculated using professional quantitative colocalization analysis software (Nikon A1; Japan) included with a Nikon A1 confocal microscope and expressed as Pearson's coefficient.

Co-IP. HEK293T cells were cotransfected with pFLAG plasmids (pFLAG-Core, pFLAG-NS2, pFLAG-NS3, pFLAG-NS4B, pFLAG-NS5A, and pFLAG-NS5B) and pcDNA3.0-poMx1-HA or pFLAG-NS5B with pcDNA3.0-poMx1-HA (mutants), pcDNA3.0-poMx2-HA, pcDNA3.0-huMxA-HA, or pcDNA3.0-mmMx1-HA (2 μg each). At 48 hpt, cells were lysed in NP-40 lysis buffer (50 mM Tris-HCl, 150 mM NaCl, 1% NP-40, 1 mM EDTA, 1 mM PMSF, 1 mM NaF, 1 mM Na_3O_4, pH 7.4) for 1 h at 4°C. To remove cell debris, the lysates were centrifuged at 10,000 $\times$ *g* for 10 min at 4°C. A 50-μl aliquot of the supernatant (the whole-cell lysate) was removed from each sample for later use. The remaining lysate was treated with 1.0 μg of the appropriate control IgG together with 20 μl of protein A/G Plus-agarose slurry (sc-2003; Santa Cruz) and incubated with rotation for 2 h at 4°C. After centrifugation at 1,000 $\times$ *g* for 5 min at 4°C, 1 μg of mouse anti-Flag MAb (F1804; Sigma-Aldrich), mouse anti-HA MAb (C1304; Applygen), or 3 μg of mouse anti-NS5B PAb (produced in our lab) was added to the supernatant, and incubation with rotation continued for 1 h at 4°C. Twenty microliters of protein A/G Plus-agarose slurry was added to each sample and incubated for another 4 h under the same conditions. The agarose beads were collected by centrifugation and washed with the NP-40 lysis buffer five times. The final pellet was dissolved in 2$\times$ SDS loading buffer for SDS-PAGE and Western blotting. Immunoprecipitations and the whole-cell lysates were probed with rabbit anti-Flag MAb (C1837; Applygen), rabbit anti-HA MAb (H6098; Sigma-Aldrich), and mouse anti-β-actin (AA128; Beyotime).

GST pulldown. poMx1 (WT and mutants) was subcloned into the pGEX-4T-1 expression vector, expressed in *Escherichia coli* BL21, and induced with isopropyl-β-D-thiogalactopyranoside (IPTG). Bacteria were harvested and suspended in cold PBS and then subjected to ultrasonication for 10 min. Subsequently, the soluble GST or GST-poMx1 (WT or mutant) fusion protein was incubated with glutathione MagBeads for 2 h at 4°C, collected by centrifugation (12,000 $\times$ *g* for 10), washed five times with cold PBS, and then incubated with the lysates of HEK293T cells transfected with 2 μg of pFLAG plasmids (pFLAG-Core, pFLAG-NS2, pFLAG-NS3, pFLAG-NS4B, pFLAG-NS5A, and pFLAG-NS5B) for 2 h at 4°C. The MagBeads were again collected and washed five times with PBS. The bound proteins were analyzed by Western blotting using mouse anti-GST MAb (A00865-100; Genscript) and mouse anti-Flag MAb (F1804; Sigma-Aldrich).

Bimolecular fluorescence complementation. Sequences encoding amino-terminal residues 1 to 173 (VN) or the carboxyl-terminal residues 174 to 239 (VC) of Venus (a variant of yellow fluorescent protein was obtained by site-directed mutagenesis of pEYFP-N1) were fused to the C terminus of the full-length or truncated N proteins via a $(GGGGS)_3$ linker (kindly provided by Ke Liu from Shanghai Veterinary Institute Research, Shanghai, China) (57). The wild-type and mutated poMx1 were cloned into VC, and NS5B was cloned into VN. The primers used for BiFC are shown in Table 1. PK-15 cells were transfected with 2 μg of plasmid (for cotransfections, 2 μg of each plasmid was used) for 20 h at 37°C, fixed with 4% paraformaldehyde in PBS, and stained with DAPI. These cells were processed for confocal microscopy as described above.

Nondenaturing PAGE. PK-15 cells were grown in six-well plates and transfected with pcDNA3.0-poMx1-HA (WT and mutants), pcDNA3.0-huMxA, pcDNA3.0-mmMx1, or pcDNA3.0 (2 μg each). Cells were lysed in NP-40 lysis buffer for 30 min at 4°C. Lysates were centrifuged at 10,000 $\times$ *g* for 10 min at 4°C, and supernatant was mixed with 10$\times$ loading buffer (12.5% 0.5 M Tris-HCl [pH 8.0], 30% glycerin, 55% double-distilled H_2O [ddH_2O], 2.5% bromophenol blue [BPB]) and run on a 6.5% separating gel in 1$\times$ Tris-borate-EDTA (TBE). Proteins were transferred to nitrocellulose and probed with rabbit anti-HA MAb (H6098; Sigma-Aldrich). Molecular weights were determined using a native protein marker (1762408; Invitrogen).

GTPase assay. The Mx-associated GTPase activities of the pHA-Mx fusion proteins expressed in PK-15 cells were analyzed using a QuantiChrom ATPase/GTPase assay kit (BioAssay Systems, USA) according to a protocol described previously (26). Briefly, PK-15 cells were washed three times with ddH_2O, and cells were suspended in ddH_2O and lysed by sonication on ice for 1 min at 2-s intervals. The lysates were centrifuged at 10,000 $\times$ *g* for 15 min, and the GTPase activity of the supernatant was examined. The change in values of the optical density at 620 (ΔOD_{620}) was calculated by subtracting OD values in the reaction product and from those of the control wells. The concentration of free phosphate produced [Pi] (in micromolars) was calculated from the part of the standard curve within the range of OD_{620} values of 0.5 to 1.0 to ensure that the substrate hydrolysis was within the linear kinetics of the reaction. Enzyme activity was calculated as follows: activity = [Pi] (μM) $\times$ 40 μl $\div$ (10 μl $\times$ *t*) (U/liter), where 40 μl is the reaction volume, 10 μl is the enzyme volume in the assay, and *t* is the reaction time. We used the enzyme activity of poMx1 (WT) protein as 100%, and then normalized the enzyme activity of other Mx1 proteins.

RNA-dependent RNA polymerase activity assay. RNA templates were total-RNA extracted from progeny viruses of the infected cell supernatant. NS5B and poMx1 (WT and mutants) were subcloned into pColdI with a His_6 tag, expressed in *Escherichia coli* BL21, and induced with IPTG. Subsequently, NS5B proteins and poMx1 proteins (WT and mutants) were purified using nickel-nitrilotriacetic acid (Ni-NTA)-Sepharose resin (L00250; Genscript). The total volume of RdRp assays was 50 μl, containing the following supplements: 50 mM HEPES (pH 8.0), 5 mM $MgCl_2$, 10 μM dithiothreitol (DTT), 25 mM KCl, 1 mM EDTA,

20 U of RNasin, 50 μg of actinomycin D, 200 μM each nucleoside triphosphate (NTP), 1 μl of RNA template (1 μg/ml), increasing amounts of NS5B proteins (0, 50, 100, 150, 200, 250, and 300 ng) or increasing amounts of poMx1 proteins (WT) (0, 50, 100, 150, 200, 250, and 300 ng) or 100 ng of NS5B proteins and 100 ng of poMx1 proteins (WT and mutants). The mixture was incubated at 37°C for 1 h, and then the reaction was stopped by the addition of 2 μl of EDTA (200 mM). The reaction samples were extracted with phenol-chloroform, and RNA was precipitated with isopropyl alcohol. Synthesized viral RNA was quantified by RT-qPCR (58, 59).

Quantification of transferrin uptake. Alexa Fluor 568 (AF568)-labeled human transferrin (Tfn) was used in uptake assays as described previously. Briefly, PK-15 cells were seeded in six-well plates and transfected with WT or mutant plasmid constructs. Cells were then incubated with 10 μg/ml of Tfn-AF568 for 30 min at 4°C and then washed and transferred to 37°C for 30 min. Cells were observed by confocal fluorescence microscopy. Total fluorescence intensity per cell was calculated using Nikon NIS-Elements AR, version 4.5, analysis software. Tfn uptake is represented as mean and standard error of the mean of integrated fluorescence intensity from two independent experiments (60).

Statistical analysis. All data are presented as means ± standard deviations (SD) as indicated in the figure legends. Student's *t* test was used to compare the data from pairs of treated or untreated groups. All statistical analyses and calculations were performed using GraphPad Prism, version 5 (GraphPad Software, Inc., La Jolla, CA).

ACKNOWLEDGMENTS

This work was supported by grants from the National Natural Science Foundation of China (31572554 and 31402180) and by Priority Academic Program Development of Jiangsu Higher Education Institutions.

We also thank Elizabeth Wills from Cornell University for critical reading and editing of the manuscript.

REFERENCES

1. Luo Y, Li S, Sun Y, Qiu HJ. 2014. Classical swine fever in China: a minireview. Vet Microbiol 172:1–6. https://doi.org/10.1016/j.vetmic.2014.04.004.
2. Moennig V, Becher P. 2015. Pestivirus control programs: how far have we come and where are we going? Anim Health Res Rev 16:83–87. https://doi.org/10.1017/S1466252315000092.
3. Rossi S, Staubach C, Blome S, Guberti V, Thulke HH, Vos A, Koenen F, Le Potier MF. 2015. Controlling of CSFV in European wild boar using oral vaccination: a review. Front Microbiol 6:1141. https://doi.org/10.3389/fmicb.2015.01141.
4. Huang YL, Deng MC, Wang FI, Huang CC, Chang CY. 2014. The challenges of classical swine fever control: modified live and E2 subunit vaccines. Virus Res 179:1–11. https://doi.org/10.1016/j.virusres.2013.10.025.
5. Pastuch-Gawolek G, Chaubey B, Szewczyk B, Krol E. 2017. Novel thioglycosyl analogs of glycosyltransferase substrates as antiviral compounds against classical swine fever virus and hepatitis C virus. Eur J Med Chem 137:247–262. https://doi.org/10.1016/j.ejmech.2017.05.051.
6. Haller O, Kochs G. 2002. Interferon-induced mx proteins: dynamin-like GTPases with antiviral activity. Traffic 3:710–717. https://doi.org/10.1034/j.1600-0854.2002.31003.x.
7. Haller O, Staeheli P, Schwemmle M, Kochs G. 2015. Mx GTPases: dynamin-like antiviral machines of innate immunity. Trends Microbiol 23:154–163. https://doi.org/10.1016/j.tim.2014.12.003.
8. Daumke O, Gao S, von der Malsburg A, Haller O, Kochs G. 2010. Structure of the MxA stalk elucidates the assembly of ring-like units of an antiviral module. Small GTPases 1:62–64. https://doi.org/10.4161/sgtp.1.1.12989.
9. Gao S, von der Malsburg A, Paeschke S, Behlke J, Haller O, Kochs G, Daumke O. 2010. Structural basis of oligomerization in the stalk region of dynamin-like MxA. Nature 465:502–506. https://doi.org/10.1038/nature08972.
10. Dick A, Graf L, Olal D, von der Malsburg A, Gao S, Kochs G, Daumke O. 2015. Role of nucleotide binding and GTPase domain dimerization in dynamin-like myxovirus resistance protein A for GTPase activation and antiviral activity. J Biol Chem 290:12779–12792. https://doi.org/10.1074/jbc.M115.650325.
11. Nigg PE, Pavlovic J. 2015. Oligomerization and GTP-binding requirements of MxA for viral target recognition and antiviral activity against influenza A virus. J Biol Chem 290:29893–29906. https://doi.org/10.1074/jbc.M115.681494.
12. Engelhardt OG, Sirma H, Pandolfi PP, Haller O. 2004. Mx1 GTPase accumulates in distinct nuclear domains and inhibits influenza A virus in cells that lack promyelocytic leukaemia protein nuclear bodies. J Gen Virol 85:2315–2326. https://doi.org/10.1099/vir.0.79795-0.
13. Hoenen A, Liu W, Kochs G, Khromykh AA, Mackenzie JM. 2007. West Nile virus-induced cytoplasmic membrane structures provide partial protection against the interferon-induced antiviral MxA protein. J Gen Virol 88:3013–3017. https://doi.org/10.1099/vir.0.83125-0.
14. Ashenberg O, Padmakumar J, Doud MB. 2017. Deep mutational scanning identifies sites in influenza nucleoprotein that affect viral inhibition by MxA. PLoS Pathog 13:e1006288. https://doi.org/10.1371/journal.ppat.1006288.
15. Mitchell PS, Young JM, Emerman M, Malik HS. 2015. Evolutionary analyses suggest a function of MxB immunity proteins beyond lentivirus restriction. PLoS Pathog 11:e1005304. https://doi.org/10.1371/journal.ppat.1005304.
16. Verhelst J, Hulpiau P, Saelens X. 2013. Mx proteins: antiviral gatekeepers that restrain the uninvited. Microbiol Mol Biol Rev 77:551–566. https://doi.org/10.1128/MMBR.00024-13.
17. Fribourgh JL, Nguyen HC, Matreyek KA, Alvarez FJD, Summers BJ, Dewdney TG, Aiken C, Zhang P, Engelman A, Xiong Y. 2014. Structural insight into HIV-1 restriction by MxB. Cell Host Microbe 16:627–638. https://doi.org/10.1016/j.chom.2014.09.021.
18. Schulte B, Buffone C, Opp S, Di Nunzio F, De Souza Aranha Vieira DA, Brandariz-Nunez A, Diaz-Griffero F. 2015. Restriction of HIV-1 requires the N-terminal region of MxB as a capsid-binding motif but not as a nuclear localization signal. J Virol 89:8599–8610. https://doi.org/10.1128/JVI.00753-15.
19. Muller M, Winnacker EL, Brem G. 1992. Molecular cloning of porcine Mx cDNAs: new members of a family of interferon-inducible proteins with homology to GTP-binding proteins. J Interferon Res 12:119–129. https://doi.org/10.1089/jir.1992.12.119.
20. Asano A, Ko JH, Morozumi T, Hamashima N, Watanabe T. 2002. Polymorphisms and the antiviral property of porcine Mx1 protein. J Vet Med Sci 64:1085–1089.
21. Morozumi T, Sumantri C, Nakajima E, Kobayashi E, Asano A, Oishi T, Mitsuhashi T, Watanabe T, Hamasima N. 2001. Three types of polymorphisms in exon 14 in porcine Mx1 gene. Biochem Genet 39:251–260. https://doi.org/10.1023/A:1010230715605.
22. Zhang XM, He DN, Zhou B, Pang R, Liu K, Zhao J, Chen PY. 2013. In vitro inhibition of vesicular stomatitis virus replication by purified porcine Mx1 protein fused to HIV-1 Tat protein transduction domain (PTD). Antiviral Res 99:149–157. https://doi.org/10.1016/j.antiviral.2013.05.009.
23. Nakajima E, Morozumi T, Tsukamoto K, Watanabe T, Plastow G, Mitsu-

hashi T. 2007. A naturally occurring variant of porcine Mx1 associated with increased susceptibility to influenza virus in vitro. Biochem Genet 45:11–24. https://doi.org/10.1007/s10528-006-9045-y.
24. Zhao Y, Pang D, Wang T, Yang X, Wu R, Ren L, Yuan T, Huang Y, Ouyang H. 2011. Human MxA protein inhibits the replication of classical swine fever virus. Virus Res 156:151–155. https://doi.org/10.1016/j.virusres.2011.01.008.
25. Zhang X, Jing J, Li W, Liu K, Shi B, Xu Q, Ma Z, Zhou B, Chen P. 2015. Porcine Mx1 fused to HIV Tat protein transduction domain (PTD) inhibits classical swine fever virus infection in vitro and in vivo. BMC Vet Res 11:264. https://doi.org/10.1186/s12917-015-0577-4.
26. He DN, Zhang XM, Liu K, Pang R, Zhao J, Zhou B, Chen PY. 2014. In vitro inhibition of the replication of classical swine fever virus by porcine Mx1 protein. Antiviral Res 104:128–135. https://doi.org/10.1016/j.antiviral.2014.01.020.
27. Yuan B, Fang H, Shen C, Zheng C. 2015. Expression of porcine Mx1 with FMDV IRES enhances the antiviral activity against foot-and-mouth disease virus in PK-15 cells. Arch Virol 160:1989–1999. https://doi.org/10.1007/s00705-015-2473-4.
28. Shi H, Fu Q, Ren Y, Wang D, Qiao J, Wang P, Zhang H, Chen C. 2015. Both foot-and-mouth disease virus and bovine viral diarrhea virus replication are inhibited by Mx1 protein originated from porcine. Anim Biotechnol 26:73–79. https://doi.org/10.1080/10495398.2014.902850.
29. Zhou J, Wang SQ, Wei JC, Zhang XM, Gao ZC, Liu K, Ma ZY, Chen PY, Zhou B. 2017. Mx is not responsible for the antiviral activity of interferon-alpha against Japanese encephalitis virus. Viruses 9:E5. https://doi.org/10.3390/v9010005.
30. Yu Z, Wang Z, Chen J, Li H, Lin Z, Zhang F, Zhou Y, Hou J. 2008. GTPase activity is not essential for the interferon-inducible MxA protein to inhibit the replication of hepatitis B virus. Arch Virol 153:1677–1684. https://doi.org/10.1007/s00705-008-0168-9.
31. Accola MA, Huang B, Al Masri A, McNiven MA. 2002. The antiviral dynamin family member, MxA, tubulates lipids and localizes to the smooth endoplasmic reticulum. J Biol Chem 277:21829–21835. https://doi.org/10.1074/jbc.M201641200.
32. Stertz S, Reichelt M, Krijnse-Locker J, Mackenzie J, Simpson JC, Haller O, Kochs G. 2006. Interferon-induced, antiviral human MxA protein localizes to a distinct subcompartment of the smooth endoplasmic reticulum. J Interferon Cytokine Res 26:650–660. https://doi.org/10.1089/jir.2006.26.650.
33. Lamp B, Riedel C, Roman-Sosa G, Heimann M, Jacobi S, Becher P, Thiel HJ, Rumenapf T. 2011. Biosynthesis of classical swine fever virus nonstructural proteins. J Virol 85:3607–3620. https://doi.org/10.1128/JVI.02206-10.
34. Spearman P. 2017. Viral interactions with host cell Rab GTPases. Small GTPases 11:1–10. https://doi.org/10.1080/21541248.2017.1346552.
35. Shi BJ, Liu CC, Zhou J, Wang SQ, Gao ZC, Zhang XM, Zhou B, Chen PY. 2016. Entry of classical swine fever virus into PK-15 cells via a pH-, dynamin-, and cholesterol-dependent, clathrin-mediated endocytic pathway that requires Rab5 and Rab7. J Virol 90:9194–9208. https://doi.org/10.1128/JVI.00688-16.
36. Nurnberger C, Zimmermann V, Gerhardt M, Staeheli P. 2016. Influenza virus susceptibility of wild-derived CAST/EiJ mice results from two amino acid changes in the MX1 restriction factor. J Virol 90:10682–10692. https://doi.org/10.1128/JVI.01213-16.
37. Pillai PS, Molony RD, Martinod K, Dong H, Pang IK, Tal MC, Solis AG, Bielecki P, Mohanty S, Trentalange M, Homer RJ, Flavell RA, Wagner DD, Montgomery RR, Shaw AC, Staeheli P, Iwasaki A. 2016. Mx1 reveals innate pathways to antiviral resistance and lethal influenza disease. Science 352:463–466. https://doi.org/10.1126/science.aaf3926.
38. Moennig V, Plagemann PG. 1992. The pestiviruses. Adv Virus Res 41:53–98. https://doi.org/10.1016/S0065-3527(08)60035-4.
39. Becher P, Thiel HJ, Collins M, Brownlie J, Orlich M. 2002. Cellular sequences in pestivirus genomes encoding gamma-aminobutyric acid (A) receptor-associated protein and Golgi-associated ATPase enhancer of 16 kilodaltons. J Virol 76:13069–13076. https://doi.org/10.1128/JVI.76.24.13069-13076.2002.
40. Pierce BG, Boucher EN, Piepenbrink KH, Ejemel M, Rapp CA, Thomas WD, Jr, Sundberg EJ, Weng Z, Wang Y. 2017. Structure-based design of hepatitis C virus vaccines that elicit neutralizing antibody responses to a conserved epitope. J Virol 91:e01032-17. https://doi.org/10.1128/JVI.01032-17.
41. Haegeman A, Vrancken R, Neyts J, Koenen F. 2013. Intra-host variation structure of classical swine fever virus NS5B in relation to antiviral therapy. Antiviral Res 98:266–272. https://doi.org/10.1016/j.antiviral.2013.03.005.
42. Musiu S, Purstinger G, Stallinger S, Vrancken R, Haegeman A, Koenen F, Leyssen P, Froeyen M, Neyts J, Paeshuyse J. 2014. Substituted 2,6-bis(benzimidazol-2-yl)pyridines: a novel chemical class of pestivirus inhibitors that targets a hot spot for inhibition of pestivirus replication in the RNA-dependent RNA polymerase. Antiviral Res 106:71–79. https://doi.org/10.1016/j.antiviral.2014.03.010.
43. Baginski SG, Pevear DC, Seipel M, Sun SC, Benetatos CA, Chunduru SK, Rice CM, Collett MS. 2000. Mechanism of action of a pestivirus antiviral compound. Proc Natl Acad Sci U S A 97:7981–7986. https://doi.org/10.1073/pnas.140220397.
44. Paeshuyse J, Chezal JM, Froeyen M, Leyssen P, Dutartre H, Vrancken R, Canard B, Letellier C, Li T, Mittendorfer H, Koenen F, Kerkhofs P, De Clercq E, Herdewijn P, Puerstinger G, Gueiffier A, Chavignon O, Teulade JC, Neyts J. 2007. The imidazopyrrolopyridine analogue AG110 is a novel, highly selective inhibitor of pestiviruses that targets the viral RNA-dependent RNA polymerase at a hot spot for inhibition of viral replication. J Virol 81:11046–11053. https://doi.org/10.1128/JVI.00388-07.
45. Paeshuyse J, Leyssen P, Mabery E, Boddeker N, Vrancken R, Froeyen M, Ansari IH, Dutartre H, Rozenski J, Gil LH, Letellier C, Lanford R, Canard B, Koenen F, Kerkhofs P, Donis RO, Herdewijn P, Watson J, De Clercq E, Puerstinger G, Neyts J. 2006. A novel, highly selective inhibitor of pestivirus replication that targets the viral RNA-dependent RNA polymerase. J Virol 80:149–160. https://doi.org/10.1128/JVI.80.1.149-160.2006.
46. Enguehard-Gueiffier C, Musiu S, Henry N, Veron JB, Mavel S, Neyts J, Leyssen P, Paeshuyse J, Gueiffier A. 2013. 3-Biphenylimidazo[1,2-a]pyridines or [1,2-b]pyridazines and analogues, novel *Flaviviridae* inhibitors. Eur J Med Chem 64:448–463. https://doi.org/10.1016/j.ejmech.2013.03.054.
47. Chen Y, Zhang L, Graf L, Yu B, Liu Y, Kochs G, Zhao Y. 2017. Conformational dynamics of dynamin-like MxA revealed by single-molecule FRET. Nat Commun 8:15744. https://doi.org/10.1038/ncomms15744.
48. von der Malsburg A, Abutbul-Ionita I, Haller O, Kochs G, Danino D. 2011. Stalk domain of the dynamin-like MxA GTPase protein mediates membrane binding and liposome tubulation via the unstructured L4 loop. J Biol Chem 286:37858–37865. https://doi.org/10.1074/jbc.M111.249037.
49. Pitossi F, Blank A, Schroder A, Schwarz A, Hussi P, Schwemmle M, Pavlovic J, Staeheli P. 1993. A functional GTP-binding motif is necessary for antiviral activity of Mx proteins. J Virol 67:6726–6732.
50. Kochs G, Haener M, Aebi U, Haller O. 2002. Self-assembly of human MxA GTPase into highly ordered dynamin-like oligomers. J Biol Chem 277:14172–14176. https://doi.org/10.1074/jbc.M200244200.
51. Verhelst J, Spitaels J, Nurnberger C, De Vlieger D, Ysenbaert T, Staeheli P, Fiers W, Saelens X. 2015. Functional comparison of Mx1 from two different mouse species reveals the involvement of loop L4 in the antiviral activity against influenza A viruses. J Virol 89:10879–10890. https://doi.org/10.1128/JVI.01744-15.
52. Kochs G, Janzen C, Hohenberg H, Haller O. 2002. Antivirally active MxA protein sequesters La Crosse virus nucleocapsid protein into perinuclear complexes. Proc Natl Acad Sci U S A 99:3153–3158. https://doi.org/10.1073/pnas.052430399.
53. Schwemmle M, Weining KC, Richter MF, Schumacher B, Staeheli P. 1995. Vesicular stomatitis virus transcription inhibited by purified MxA protein. Virology 206:545–554. https://doi.org/10.1016/S0042-6822(95)80071-9.
54. Morozumi T, Naito T, Lan PD, Nakajima E, Mitsuhashi T, Mikawa S, Hayashi T, Awata T, Uenishi H, Nagata K, Watanabe T, Hamasima N. 2009. Molecular cloning and characterization of porcine Mx2 gene. Mol Immunol 46:858–865. https://doi.org/10.1016/j.molimm.2008.09.019.
55. Sasaki K, Tungtrakoolsub P, Morozumi T, Uenishi H, Kawahara M, Watanabe T. 2014. A single nucleotide polymorphism of porcine MX2 gene provides antiviral activity against vesicular stomatitis virus. Immunogenetics 66:25–32. https://doi.org/10.1007/s00251-013-0745-2.
56. Livak KJ, Schmittgen TD. 2001. Analysis of relative gene expression data using real-time quantitative PCR and the $2^{-\Delta\Delta CT}$ method. Methods 25:402–408. https://doi.org/10.1006/meth.2001.1262.
57. Liu K, Feng X, Ma Z, Luo C, Zhou B, Cao R, Huang L, Miao D, Pang R, He D, Lian X, Chen P. 2012. Antiviral activity of phage display selected peptides against porcine reproductive and respiratory syndrome virus in vitro. Virology 432:73–80. https://doi.org/10.1016/j.virol.2012.05.010.

58. Xiao M, Gao J, Wang W, Wang Y, Chen J, Chen J, Li B. 2004. Specific interaction between the classical swine fever virus NS5B protein and the viral genome. Eur J Biochem 271:3888–3896. https://doi.org/10.1111/j.1432-1033.2004.04325.x.
59. Wang Y, Zhu Z, Wang P, Yu J, Wan L, Chen J, Xiao M. 2011. Characterisation of interaction between NS3 and NS5B protein of classical swine fever virus by deletion of terminal sequences of NS5B. Virus Res 156:98–106. https://doi.org/10.1016/j.virusres.2011.01.003.
60. Kalia M, Khasa R, Sharma M, Nain M, Vrati S. 2013. Japanese encephalitis virus infects neuronal cells through a clathrin-independent endocytic mechanism. J Virol 87:148–162. https://doi.org/10.1128/JVI.01399-12.